Electronic Theses and Dissertations

Theses, Dissertations, and Major Papers

1-1-2006

Characterization of the catalytic properties of dual specificity protein tyrosine phosphatase hYVH1.

Khaled Elmosrati
University of Windsor

Follow this and additional works at: https://scholar.uwindsor.ca/etd

CHARACTERIZATION OF THE CATALYTIC PROPERTIES

OF DUAL SPECIFICITY PROTEIN TYROSINE

PHOSPHATASE hYVH1

by

KHALED ELMOSRATI

A Thesis
Submitted to the Faculty of Graduate Studies and Research
through Chemistry & Biochemistry
in Partial Fulfillment of the Requirements for
the Degree of Master of Science at the
University of Windsor

Windsor, Ontario, Canada

© 2006 Khaled Elmosrati

NOTICE:
The author has granted a non-exclusive license allowing Library and Archives Canada to reproduce, publish, archive, preserve, conserve, communicate to the public by telecommunication or on the Internet, loan, distribute and sell theses worldwide, for commercial or non-commercial purposes, in microform, paper, electronic and/or any other formats.

AVIS:
L'auteur a accordé une licence non exclusive permettant à la Bibliothèque et Archives Canada de reproduire, publier, archiver, sauvegarder, conserver, transmettre au public par télécommunication ou par l'Internet, prêter, distribuer et vendre des thèses partout dans le monde, à des fins commerciales ou autres, sur support microforme, papier, électronique et/ou autres formats.

The author retains copyright ownership and moral rights in this thesis. Neither the thesis nor substantial extracts from it may be printed or otherwise reproduced without the author's permission.

L'auteur conserve la propriété du droit d'auteur et des droits moraux qui protège cette thèse. Ni la thèse ni des extraits substantiels de celle-ci ne doivent être imprimés ou autrement reproduits sans son autorisation.

In compliance with the Canadian Privacy Act some supporting forms may have been removed from this thesis.

Conformément à la loi canadienne sur la protection de la vie privée, quelques formulaires secondaires ont été enlevés de cette thèse.

While these forms may be included in the document page count, their removal does not represent any loss of content from the thesis.

Bien que ces formulaires aient inclus dans la pagination, il n'y aura aucun contenu manquant.

Canada

ABSTRACT

The human YVH1 is a dual specific protein tyrosine phosphatase (DUS PTP) that was identified in 1999 as an orthologue of the *Saccharomyces cerevisiae* YVH1 and found to be highly expressed in human tissues. The human yvh1 gene maps to chromosome Iq-21-q23, which is amplified in human sarcomas. Using the *in vitro* assay we determined the kinetic parameters of hYVH1 towards synthetic substrates, OMFP and DiFMUP. Also using these substrates and pH dependency experiments we demonstrated that hYVH1 obeys the PTP catalytic mechanism. Kinetic analysis of wild type hYVH1, D84A, and D98 at different pH conditions led to the identification of the catalytic acid/base residue, D84. Also, we identified a novel critical residue for acid/base catalysis, D89, that stabilizing the function of D84. Notably, this novel residue was found to be conserved in dual specific MKPs subfamily. This study provides valuable tools to study catalytic regulation of hYVH1 in the future.

DEDICATION

To my mother (Najat), wife (Fatma),

son (Omar), and daughter (Noor Elhoda).

iv

ACKNOWLEDGEMENTS

I would like to express my gratitude to my thesis advisor, Dr.Panayiotis Vacratsis, for his guidance and support during all the period I spent in his lab. Our numerous scientific discussions and his many constructive comments have greatly improved this work. I wish him all success and prosperity.

I would also like to thank Dr. Jerald Lalman and Dr. Ananvoranich for their accepting to be members in my committee. I am also grateful to Dr. Ananvoranich, Dr. Mutus, Dr. Lee, and Dr. Pandy for allowing me to use their laboratory instruments. In addition, I would like to thank Marelen Bezaire, Elizabeth Kickham, and Kimberly Kickham for their assistance in administrative issues. They were always friendly and willing to give advices and help.

My gratitude is due to the administration of scholarships and technical cooperation department of The Ministry of Education of my country, Libya; which financially covered my living expenses, tuition fees, and health care costs during all my stay in Canada. Along with the cultural department of Libyan embassy in Canada, that is organizing and processing the Libyan Scholarships Program.

My thanks are extended to every member of Dr. Otis' lab: Katherine Sykes, Priya Sharda, John Mucaki, Anna Kozarova for their being so cooperative, friendly, and supportive; I consider the period I spent with them is unforgettable period in my life.

Special thanks to Ahamad Elryahi, Walid Elgherwi, Inga Sliskovic, Arun Raturi

for not only their help in scientific matters but also for being such a good company; also, "Thank you" to every one in Department of Chemistry and Biochemistry.

Last but not least, I would like to express my deep appreciation to my wife, Fatma Ali, for her priceless support and constant patience particularly that related to taking care of our children, Omar and Noor. As a small family they made my life in Canada easier and enjoyable.

TABLE OF CONTENTS

viii

LIST OF TABLES

x

LIST OF FIGURES

xi

LIST OF ABBRIVIATIONS

ATP	Adinosine triphosphate
DiFMUP	di-Fluoro-4-methylumbelliferyl phosphate
DMSO	Dimethylsulfoxide
DNA	Deoxyribonucleic acid
dNTP	Deoxyribonucleotide triphosphate
DTT	Dithiotheritol
DUS	Dual specific
EDTA	Ethyldiamintetraacetate
GST	Glutathione-S-transferase
HEK Cells	Human Embryonic Kidney cells
IPTG	Isopropyl-β-D-thiogalactopyranoside
LB media	Luria-Bertani media
MAPK	Mitogene activated proteine kinase
MKP	Mitogene activated proteine kinase phosphatase
OMF	*ortho*-Methylfluorescein
OMFP	*ortho*-Methylfluorescein phosphate
PCR	Poly chain reaction
pNP	*para*-Nitrophenyl
pNPP	*para*-Nitrophenylphosphate
PS/TP	Protein serine/threonine phosphatase
PTP	Protein tyrosine phosphatase
RFU	Relative fluorescence units
RNA	Ribonucleic acid
SDS-PAGE	Sodium dodecyl sulphate – polyacrylamide gel electrophoresis
TBS	Tris bis-tris saline

xiii

CHAPTER 1

INTRODUCTION

1.1 Cellular Phosphorylation

Reversible phosphorylation is a major strategy that is widely utilized by living cells, from prokaryotes to eukaryotes, to regulate proteins and control their functions (1). Proteins are post-translationally modified by the transfer of a γ-phosphoryl group from an ATP molecule by a protein kinase to the hydroxyl side chain of, serine, thereonine and tyrosine residues in eukaryotes, or histidine and aspartate residues in prokaryotes (2). The covalent binding of the phosphoryl group (phosphorylation) to the side chain substantially changes the tertiary and/or quaternary structure and consequently the biochemical properties of the modified protein. This is due to the double negative charge on the phosphoryl group along with its ability to function in multiple-hydrogen bonding interactions. Likewise, the removal of a phosphoryl group (dephosphorylation) from the protein by a protein phosphatase reverses the changes that occurred by the phosphorylation event. Such reversible processes are widely used in cellular signalling, where this highly balanced and harmonized phosphorylation is involved in many diverse cellular processes including intracellular membrane trafficking, cell cycle progression, cellular proliferation, differentiation, development, metabolic pathways, gene transcription regulation, as well as viral and bacterial pathogenicity (3).

However, within this network, the biological activities of protein kinases and protein phosphatases, themselves, are often regulated by phosphorylation. Hence,

1

disturbances in any of these network processes, whether by environmental signals or genetic alterations, frequently result in a dysfunction that may develop into a serious pathological condition such as malignancies, hypoplasia, neurodegenerative diseases, metabolic and immune disorders (3,4,5).

1.2 Protein Kinase and Protein Phosphatase Specificity

Protein kinases are a class of enzymes that catalyze the phosphorylation of either serine/thereonine or tyrosine residues. The specificity of this class mostly depends on a consensus sequence within their substrates which is mainly directed by hydrophobic forces and/or ionic bonds. However, protein kinases usually have more than a single protein substrate. Rather, their specificity covers common recognition sequences through a whole protein family (4).

Protein kinases, including serine/thereonine and tyrosine kinases, share common amino acid sequence motifs, and consequently, common secondary and tertiary folds. This undoubtedly implies that they evolutionary descended from one genetic origin. In contrast, protein serine/thereonine phosphatases have no structural or mechanistic similarity with protein tyrosine phosphatases. Moreover, while the protein kinases are encoded by more than 400 genes in the human genome, only approximate 100 phosphatases are present. This disparity can be explained by the fact that proteins are continuously down-regulated by degradation in their phosphorylated forms with no need to be dephosphorylated **(Fig. 1)**. This also suggests more multiplicity in specificity and/or functionality of phosphatases in balancing 4 times-folds the number of kinases (6, 7).

2
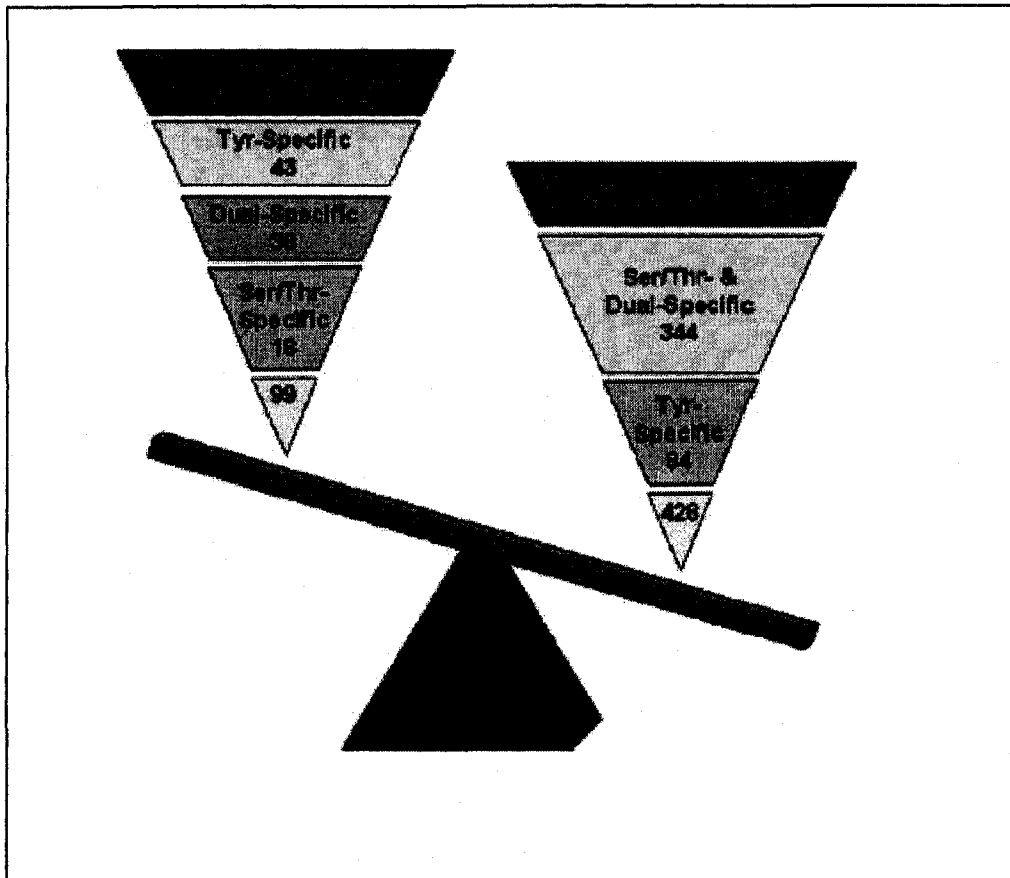
Figure 1: Balance of protein kinases and phosphatases in the human genome.

This figure is adapted from a review written by (Alexander *et al,*.2005) (6)

3

1.3 Categorization of Protein Tyrosine Phosphatases

Protein Phosphatases are categorized according to their substrate specificity; either serine/thereonine phosphatases (PS/TPs) or tyrosine phosphatases (PTPs). PS/TPs catalytic mechanism involves dephosphorylation of their substrates in one step using a metal-activated water molecule or hydroxide ion (4). In contrast, the PTPs are characterized by the presence of the evolutionary-conserved active site signature motif, $C(X)_5R$, and the catalytic mechanism that includes the formation of a phospho-enzyme intermediate complex. The PTP superfamily is categorized into three main subfamilies: Classical PTPs, dual specific PTPs, and lipid specific PTPs.

The classical PTPs can be subdivided according to their intracellular localization as a receptor-like and non-receptor-like. This is directly related to the presence of extracellular and transmembrane regions. Receptor-like PTP consists of a transmembrane domain in addition to variable extracellular domain(s). CD45 is an example of receptor-like PTPs, also known as leukocyte common antigen (LCA). CD45 has been determined to be important for activation of T and B lymphocytes via their antigen-specific receptor (8 – 10). The non-receptor PTPs category involves all the classical PTPs that have a single or multiple cytoplasmic domains and are specific only to phospho-tyrosine substrates. PTP1 is a well-studied member of classical non-receptor PTPs. It has shown to dephosphorylate and regulate several kinases, including the insulin response kinase (IRK) that negatively regulates insulin signalling (8, 11, 12). Another class of classical PTPs are termed the low-molecular weight PTPs. Although this class has different substrate targets and a lower molecular weight than the other PTPs, it has a high

4

similarity within the active site suggesting a highly similar catalytic mechanism (13 – 17).

The PTPs had been believed to be all strictly tyrosine-specific until Guan *et al.*, (1991) identified the first protein phosphatase encoded by the vaccinia virus (VH1) open reading frame that contains the signature motif of PTP superfamily, $C(X)_5R$. and was found to be able to hydrolyze phospho-serine/thereonine in addition to phospho-tyrosine (18). By this discovery, a new subfamily of PTPs has emerged and is termed Dual Specificity Protein Tyrosine Phosphatase, (DUS-PTP). Currently, the dual specificity PTPs family is increasingly growing involving a wide range of enzymes such as VH1-like DUS PTP, phosphatase of regenerating liver (PRL), CDC25, and MKPs. The mitogen-activated protein kinase phosphatase (MKP) family is classified based on their specificity towards mitogen-activated protein kinases (MAP kinases) and thus play critical roles regulating cell proliferation, cell cycle progression and cellular survival (6).

The lipid specific PTPs are also grouped with the dual specific PTPs, but they represent a unique subfamily because of there high specificity towards phosphoinositol lipids. PTEN, an example for this family, is reported to play an essential role in cell cycle division, apoptotic signalling pathways, and it is well-known as a tumour suppressor protein (5).

1.4 Structural Features of PTPs

Numerous published studies have focused on solving the three dimensional structure of PTP superfamily members, and its relation with the catalytic mechanism of PTPs (11, 13, 19 – 22). The results have shown that although classical PTP, dual specific, and other PTP superfamily members have a low percentage of primary sequence

5

similarity, they share relatively high similarity in secondary and tertiary structure within the catalytic domains.

The tertiary structure of the catalytic domain is rich in beta sheets with helices surrounding the PTP signature motif $C(X_5)R$. Although, this signature motif has been found to be located at varied positions within catalytic domains of PTPs, the structure of surrounding region where it locates, in general, is highly similar (5,23). Within the structure of the active site there are several loops that play important roles in catalysis and substrate specificity. The loop that contains the signature motif of PTP superfamily is termed the P-loop. An additional loop contains the invariant Asp residue necessary for acid-base catalysis. This loop is termed the WPD loop because it contains a highly conserved Trp, Pro, and Asp residues. However, the WPD loop is featured only in members of the classical PTP family. The catalytic acid loop has been found to move upon binding between substrate and the catalytic loop into the position where it can function as a catalytic acid. For example, crystallography studies, by Jia *et al.*, (1995), have demonstrated that PTP1B, with binding to a phospho-peptide or pTyr, undergoes a conformational change in the WPD loop that contains residues from W179 to S187. The D181 side chain is shifted by 8Å towards the binding point between active site and phosphate group of the substrate (24).

1.5 Catalytic Mechanism of PTPs

The catalytic mechanism of PTP superfamily consists of the following three steps; Nucleophilic catalysis, acid catalysis, and base catalysis. The first step involves a nucleophilic attack by a cysteine thiolate anion which attacks the substrate's phosphate group and covalently binds to the phosphate forming an enzyme-phospho-substrate

6

intermediate. Upon the binding between the phospho-substrate and the catalytic cysteine, a general acid residue, usually Asp, protonates the oxygen of substrate and facilitates the dephosphorylated product to leave from the active site. The same Asp residue then acts as a catalytic base to abstract a proton from a water molecule which in turn attacks the phosphate and induces the release of inorganic phosphate group and the recovery of the active site (Fig. 2).

1.5.1 - Catalytic Cysteine Determination:

The characterization of the catalytic mechanism of PTPs started with the observations reported in 1988 about the role of sulfhydryl-reducing agents in PTPase activity (25 – 27). This observation implicated the involvement of a cysteine group in the catalytic mechanism of PTPases. Shortly thereafter, Streuli et al., (1990) confirmed a critical role of Cys828 in the catalytic activity of CD45, as the phosphatase activity was completely abolished with substitution of this cysteine by serine (23,28).

Numerous reports supported the pivotal role of a Cys in PTPase mechanism (29-31). Further studies have shown that this catalytic cysteine and some of its invariant-adjacent residues. The histidine, for instance, was found to participate, significantly but not essentially, in PTPase activity (32). Furthermore, using ^{32}P-labeled substrates, Dixon's group demonstrated that the covalent binding between the phosphate group of the substrate molecule and the catalytic cysteine occurred due to the nucleophilic attack of the cysteine thiol group (32, 33). This interaction, compared to previous studies, signified that the mechanism of PTPase was distinct compared to other phosphatase such as alkaline/acid phosphatases and protein serine/thereonine phosphatase (8 – 10, 32).

7

A great deal of work subsequently has proven that the catalysis of PTPase starts with the nucleophilic attack by a catalytic cysteine residue with which the phosphoryl group being displaced from the substrate to the cysteine-thiol group forming a phosphoenzyme intermediate complex, which in turn is hydrolyzed by H2O. Further studies, using site directed mutagenesis, have elucidated the roles of other residues adjacent to the catalytic cysteine residue (Fig. 3). Details of these studies are discussed below:

1.5.2 – The Invariant Arginine:

The invariant Arg is located on the highly conserved CX_5R motif, which in turn is located on the catalytic loop around the catalytic cysteine. This invariant Arg was first demostrated to be involved in the catalytic mechanism in CD45 (23, 34). In another study, Cirri *et al.*, (1993) observed that mutation of the Cys or the Arg in the CX5R motif abolished the phosphatase activity of Low-molecular-weight protein tyrosine phosphatase (14). However, it was not clear what role this conserved Arg played in the catalytic mechanism until Zhang *et al.*, (1994) (35) studied the effect of altering R409 on the catalytic properties of *Yersinia* PTP. The mutant form, R409A showed a severe decrease in k_{cat} and a substantial increase in K_m. Interestingly, comparing activity of R409A to R409K resulted in that the latter mutant having a 13-fold higher K_m than that of R409A. These studies as well as numerous crystallographic studies pointed out to a role for the Arg residue in neutralizing the negative charges on the phosphate ion in the active site.

1.5.3 – The Invariant Serine/Thereonine:

Another important residue that has been elucidated to be nearly invariant in the catalytic loop is a Ser/Thr residue immediately

8
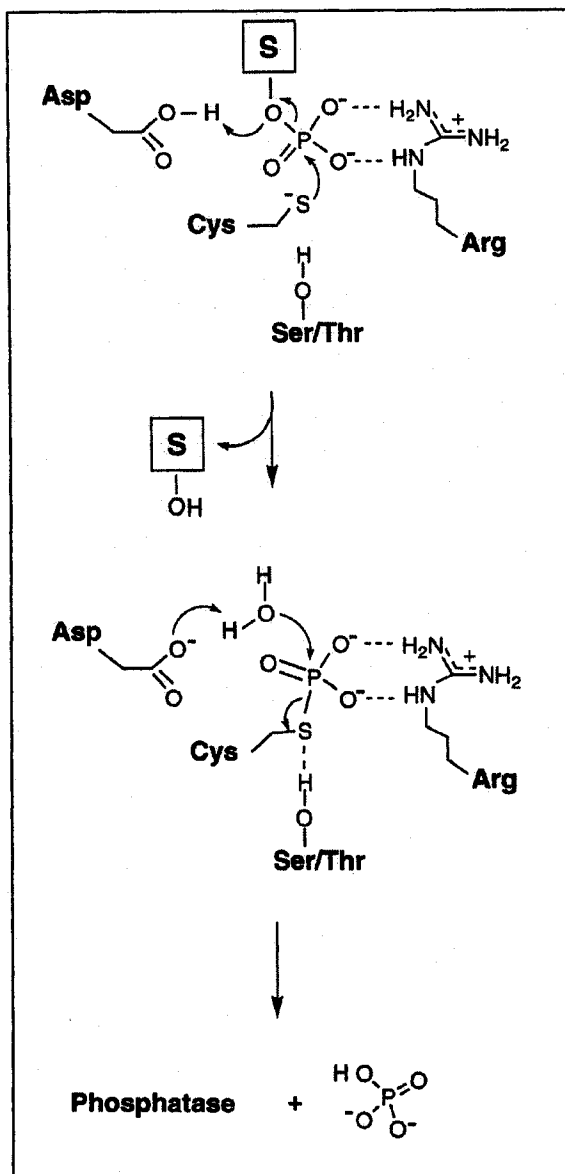
Figure 2: Catalytic mechanism of the superfamily, protein tyrosine phosphatease.

In the first step the phospho-substrate binds to the active site of the enzyme; the graph shows the hydrogen bonding of the side chain of invariant Arg with the two ionized oxygen molecules on the phosphatase group. The thiol anion nucleophilically attacks the phosphate group, and the catalytic acid donates a proton to the phosphorylated product. The second step includes the catalytic base enhancing the leaving of phosphate group from the enzyme active site through activation of the hydroxyl ion and the recovery of the enzyme.

9

```
L.M.W-PTP    11  V │C│ L  G  N  I  C  R  S

PTP1B       214  H │C│ S  A  G  I  G  R  S

hYVH1       114  H │C│ H  A  G  V  S  R  S

VHR         123  H │C│ R  E  G  Y  S  R  S
```

Figure 3: An alignment within the P loop for four distinct members of the protein tyrosine phosphatase superfamily.

adjacent to the CX₅R motif. Comparative experiments, using pre-steady state stopped-flow assays, between wild type and S/T to Ala mutants of PTPases have demonstrated a significant role for this residue in phospho-enzyme breakdown. It is believed that the hydroxyl group stabilizes the catalytic thiolate anion through a hydrogen bond (12,15,36-39). This effectively promotes the breakdown of the final phospho-enzyme intermediate.

1.5.4 - Acid/base Catalysis:

General acid/base catalysis is involved in releasing the dephosphorylated product and regenerating the phosphatase active site. Following formation of the enzyme-substrate complex, the general acid donates a proton that causes the bond between the phosphate ion and the substrate's side chain to weaken. Subsequently, the Asp residue then acts as a general base against a water molecule which in turn attacks the cysteinyl-phosphate intermediate. The nucleophilic attack of the water breaks the bond between catalytic Cys and phosphate. The catalytic cysteine and the catalytic acid is then recovered and ready to begin hydrolyzing a new phospho-substrate molecule.

General acid/base catalysis in PTPase can be observed by the bell-shaped k_{cat} versus pH profile, and substitution of the Asp residue results in substantial lower activity with no pH dependency. The pivotal study was done by Zhang *et al.,* (1994) (40) when he examined the catalytic properties of *Yersinia* PTPase (Yop51). This enzyme demonstrated a pH-dependency which suggested the presence of two ionized residues contributing to *Yersinia* PTP-catalyzed reaction. In other words, this observation suggested that the PTP catalyzed reaction involves general acid/base catalysis. Because of the pKa values in the bell-shaped curve of pH profile were in between 4.6 and 5.2, which is the range of ionization of Asp, Glu, or His residues, Zhang *et al.* and Guan &

Dixon (1990) (41) searched for invariance of these residues in the PTP superfamily. They implicated one invariant His and seven acidic residue (Asp or Glu); using site directed mutagenesis they examined how alteration of these residues affected the catalytic properties. The pH dependency for the mutant forms of Yop51 resulted in determining that Asp356 and Glu290 were responsible for the acid and base catalysis respectively (42). This result was shortly supported by other studies. The low-molecular weight phosphatase, Bovine heart phosphotyrosyl phosphatase (BHPTP) proved to have an Asp129 residue, located on a movable loop, which is involved in the catalytic activity of the enzyme. This role was confirmed by site directed mutagenesis and catalytic assays towards the artificial substrate para-Nitrophenylphosphate (pNPP) (16,17,43).

The dual specificity phosphatase VHR and protein tyrosine phosphatase PTP1 have also shown similar results confirming the necessity of the general acid/base catalytic residue. However, although the detailed mechanism of acid base catalysis of Asp is established for most of PTPs, in certain cases, exceptions in the details of catalytic mechanism can exist.

Yop51, for example, has interestingly shown an acid/base catalysis contributed by two residues (E290 and D356) in contrast of what is known in the classical PTPs of eukaryotic cells (42). The other exception is CDC25B which has shown a pH-independent manner of catalytic activity towards artificial substrates such as pNPP and 3-ortho-methylfluorescienphosphate (OMFP), which indicates that the phosphatase activity towards these substrates can proceed with out acid catalysis, whereas the pH-dependency was evidently observed with its physiological substrate, cyclin-CDK substrate. This observation led to the suggestion that CDC25 uses different mechanism in which the

12

substrate provides the proton to the leaving group, while the catalytic base residue (E474) resides on the enzyme (44 – 46).

1.6 Dual Specificity Protein Tyrosine Phosphatase

The dual specificity protein tyrosine phosphatases (DUS-PTP) family is a subcategory of the PTP superfamily in accordance with structural similarity and the presence of the PTPase active site motif as well as employing the same catalytic mechanism. However, the dualism of specificity refers to its ability to hydrolyze p-S/T in addition to p-Y substrates. Structural analyses have referred this ability to the shallower depth of the active site cleft, in which phospho-thereonine/serine can reach the bottom of the active site (22, 47)

DUS-PTP is an increasingly-growing family, as new members have been being identified annually. DUS-PTPs are reported to play pivotal roles in a wide range of signalling pathways such as cell-cycle division, cell death, cellular proliferation, and hormonal cellular response (6). With more than 50 members, the DUS-PTP subfamily is subdivided into the following five groups: VH1-like, MKPs, Cdc14-like phosphatases, Phosphoinositide phosphatases and mRNA 5'-triphosphatases. The VH1-like group emerged with the identification of VH1, the DUS PTPase encoded by the *Vaccinia* virus and is found to play an essential role for Vaccinia virus life cycle (18). Interestingly several VH1 orthologues have been identified in other related viruses such as thopoxviruses and a baculovirus (48).

1.7 YVH1 PTP, The *Saccharomyces cerevisiae* Homoluge of VH1

Exploring the possibility of finding counterparts to the VH1 DUS-PTP in eukaryotic cells, Guan and his coworkers (1992) searched in yeast cells genes and found

13

a yeast homologue for VH1 termed YVH1 (also known as DUSP12). It was the first eukaryotic dual specific protein phosphatase classified (49). YVH1 possesses a catalytic N-terminus domain that contains all the critical residues for PTPase activity, although, crude activity studies apparently showed low levels of activity towards artificial substrates that have long been widely used as models for detecting phosphatase activity (50).

YVH1 gene was found to be dramatically induced due to nitrogen starvation. This induction is specific for the nitrogen starvation and not the carbon starvation (49). The Deletion of YVH1 gene caused defects in sporulation and glycogen accumulation and resulted in a slow growth phenotype (50,51). This implicated YVH1 in regulation of sporulation, growth, and glycogen accumulation *in Saccharomyces cerevisiae*, but independent of its supposed phosphatase activity, since the catalytic cysteine deletion mutant was able to maintain the inhibitory effect of YVH1 on slow growth phenotype that induced by YVH1 gene disruption.

The C-terminus domain encods two zinc finger motifs (52). The zinc finger motifs are known to be the binding sites towards other interacting proteins, DNA or RNA (53). Muda et al. (1999) suggested that the zinc finger domain in YVH1 is dispensable for *in vitro* phosphatase activity, but was essential for function *in vivo*.

The catalytic domain of YVH1 was reported to bind to the Yeast *Pescadillo* Homolog, YPH1, which is an essential regulator for cell cycle progression, in a yeast two hybrid screen (54). This study suggested that YPH1 acts downstream of YVH1 in vegetative growth and sporulation, and is a substrate candidate or a regulatory subunit of YVH1. However, no functional significance of this interaction has been reported yet. A

14

more recent study has identified an YVH1 orthologue in *Plasmodium falciparum*, the causative agent of the malignant form of malaria, and named it PfYVH1 (54). This study has supported results of former studies particularly that related to the role of the zinc finger domain in complementing the ΔYVH1 slow-defected growth, and the interaction of PfYVH1 with the pescadillo ortholog in *P. falciparum* (PfPES) (55).

1.8 *hYVH1*, The Human Ortholgue of YVH1

The human orthologue of YVH1 was identified in 1999 by Muda *et al.*, and was found to share an over all identity of 31% with the YVH1 sequence. hYVH was determined to consist of two domains with a molecular weight of 37,690 Da. The N-terminal domain primary sequence was found to possess all the catalytically critical residues for dual specificity protein tyrosine phosphatase.

The C-terminal domain was determined to have a novel Cys-rich motif which was also present in *Saccharomyces cerevisiae* YVH1 and *S. pombe* YVH1, as well as in *P. falciparum*. This motif is composed of seven invariant cysteines and one histidine. Using inductively coupled plasma atomic emission spectroscopy (ICP) Muda *et al.*, quantified the metal species bound to the purified wild type GST-hYVH1 as well as GST-hYVH1ΔC (C-term. deletion mutant). The ICP assay demonstrated that hYVH1 does specifically contain 2 moles of zinc per mole of protein whereas the GST-hYVH1ΔC contained no zinc or other metals (52).

At the level of mRNA, hYVH1 was detected in most human tissues with the highest expression level in spleen, testis, ovary and leucocytes; and the lowest expression in lung and liver. Furthermore, using western blot technique with hYVH1-antisera the protein was found to be expressed in variety of cell-lines.

1.9 Objectives

The hYVH1 DUS PTP is an enzyme that is widely expressed in human tissues. YVH1 orthologues are structurally highly conserved in eukaryotes. It has been shown that orthologues can complement one another in gene deletion experiment suggesting that their biological function is conserved as well. YVH1 enzymes also are predicted to have a role in cellular growth, sporulation, and glycogen accumulation, although nothing is known about their precise biological role. Interestingly, a recent report found that the hYVH1 gene is amplified in various malignant sarcomas highlighting the importance of studying hYVH1 properties. Although the human orthologue of YVH1 was identified in 1999, there is no information reported on its physiological role in human cells. This has been largely due to lacking of knowledge of its physiological substrate, regulation, or catalytic properties. The purpose of this study is to examine the enzymatic properties of hYVH1.

The specific objectives of this study are:

1. To develop an efficient protocol for large scale expression and purification of GST tagged hYVH1 in bacterial cells.

2. To measure kinetic parameters of hYVH1 and confirm that hYVH1 obeys the catalytic mechanism of PTPs including the general acid/base catalysis stage.

3. To establish *in vitro* and *in vivo* phosphatase assays with which the catalytic properties of hYVH1 under various conditions can be studied.

17

CHAPTER – 2

MATERIALS AND METHODS

2.1 Site Directed Mutagenesis

PCR-based site directed mutagenesis was carried out using the following oligonucleotides constructed by *(Invitrogen)*: D74A (5'- cct ggg gtc gag gct-ctatggcgcc-3'), and D89A (5'cccgagacggccctactcagccatctg-3'). Using (Techgene) thermocycler the PCR procedures were performed in a 50 μL volume of reaction and optimized for each primer separately as following:

D74A: 5 μL reaction buffer, 1.0 μL MgSO$_4$, 3.5 μL x 0.065 μg/μL Template DNA, 1.5 μL (0.5 μM final conc) forward primer, 1.5 μL (0.5 μM final conc) Reverse primer, 1.5 μL (0.3 μM final Conc) dNTP, 2.5 μL enhancer buffer, 0.75 μL polymerase Pfx (Invitrogen), 32.75 μL autoclaved Millipore water.

D89A: 5 μL reaction buffer; 1.0 μL MgSO$_4$; 2.5 μL x 0.065 μg/μL template DNA; 3 μL (0.5 μM final conc) forward primer; 3 μL (0.5 μM final conc) Reverse primer; 1.5 μL (0.3 μM final Conc) dNTP, 2.5 μL enhancer buffer, 0.75 μL Pfx DNA-polymerase, 30.75 μL autoclaved Millipore water.

Thermal cycling was conducted as following:

18

Disruption of the YVH1 gene in yeast cells strikingly increased the doubling time of yeast cells, resulting in a so-called slow growth phenotype. Interestingly, insertion of a centromeric yeast expression vector expressing the hYVH1 gene could restore the normal growth phenotype of yeast cells (56). This observation suggested that the function of hYVH1 was conserved over the vast evolutionary period between yeast and mammalian species. In addition, this functional conservation suggests that YVH1 orthologues play a fundamental role in eukaryotic cells in general. Furthermore, according to Muda *et al.*, the zinc finger domain is essential for hYVH1 function *in vivo*, since the expression of the truncated catalytic domain, hYVH1ΔC, could not complement the disruption of YVH1 gene in yeast cells.

The hYVH1 maps to chromosome 1q-21-q23, which was observed by Forus *et al.*,(1995, 1998) (57, 58) to be amplified in human sarcomas. Interestingly, consistent with this observation, Kresse *et al.*,(2005) (59) studied 10 cases of sarcoma samples to explore and map the amplicon in the region 1q23. The hYVH1 gene was found to be the higher one of two genes that were highly amplified in these malignant sarcomas, suggesting that hYVH1 overexpression could be involved in the formation of certain sarcomas.

16

	D74A	D89A	time
Initial denaturing temperature	95°C	95°C	2 min (one time)
Denaturation step temperature	95°C	95°C	30 S
Annealing step temperature	55°C	60°C	40 S
Extension step temperature	72°C	72°C	6 min (25 times)
Final extension step temperature	72°C	72°C	10 min (one time)

PCR product was analyzed on 1% agarose gel and then subjected to Dpn I digestion at 37°C for 2 hours to eliminate parental DNA.

2.2 Preparation of Highly-Competent Cells, *DH5α-E.coli*

DH5α strain of *E.coli* was inoculated on *Luri-Bertani* (LB) agar plate (consisting of 10g/L tryptone, 5 g/L yeast extract, 5 g/L NaCl, 15 g/L and 0.1 g/L tetracycline). A single colony was selected and inoculated into 5 mL of LB medium containing 0.1 g/L tetracycline, and incubated at 37°C with a shaking speed 250 rpm for 16 hours. One mL of grown culture was inoculated into 200 mL of LB media that contained no antibiotics and incubated with shaking at 250 rpm and 37°C. The culture was harvested when the optical density was approximately 0.3 at 600 nm. The 200 mL culture was aliquoted into four 50 mL conical tubes (Falcon) chilled on ice for 30 min and then spun down at speed of 3000 rpm in a swinging bucket rotor for 15 minutes at 4°C. An approximate 45 mL of each tube was discarded and the pellets were resuspended in the remaining 5 mL. The

19

suspensions were washed with 40 mL ice-cold sterile 100 mM CaCl$_2$ solution and promptly spun down at 3000 rpm and 4°C for 15 minutes. The washing step as repeated 3 times followed by resuspending each pellet in 1.0 mL of ice-cold 200 mM CaCl$_2$ containing 15% sterile glycerol. The suspensions were dispensed into 150 μL in sterile 1.5 mL tubes (Eppendorf). Tubes were immediately and individually loaded on dry ice and stored at -80°C. The competency of cells was tested after 48 hours of storing with transformation of cells using 1.0 μL (50ng/μL) of *pGEX-4T1* plasmid.

2.3 Transformation and DNA Purification

Highly competent DH5α–*E.coli* or BLR-*E.coli* aliquots were thawed on ice and loaded with 10 μL of the PCR product or purified plasmid *(pGEX-4T1 or pCMV)*. One aliquot of cells, that was not added DNA, was used as a control. The mixture was left on ice to settle for 30 minutes and then heat-shocked at 42°C for 2 minutes promptly followed by chilling cells on ice for at least 5 minutes. The transformed cells were incubated at 37°C after adding 500 μL of sterile LB for one hour and then reconcentrated to 150 μL. Cells were resuspended and spread on LB agar containing100 μg/mL and incubated overnight (up to 16 hours). Colonies were selected from the plates and inoculated with 5 mL of LB medium. For cells that were transformed with PCR products, the DNA was purified using a mini prep kit (Sigma), visualized on 1% agarose gel and then sent for automated sequencing (ACGT, Inc).

2.4 Protein Expression and Purification in Bacterial Cells

cDNA encoding hYVH1 inserted into *pGEX.4T1* vector was used to transform BLR strain of *E.coli* and a small culture was started from a single colony, followed by inoculation in 500 mL of culture media. Bacterial cells were inoculated in conventional LB, 2XYT and 2XYT + 1.0% glycerol. Cultures were grown up to 1.0 (OD) at 600 nm. Isopropyl-beta-D-thiogalactopyranoside (IPTG) was then added to a concentration of 0.8 mM to induce expression of the fusion protein at room temperature overnight with a shaking speed of 250 rpm. Cells were spun down at 4°C, supernatant was discarded and the pellet was resuspended in and then sonicated in 20 mL of the lysis buffer (10m Tris, 150 mM NaCl, 1.0 % Tritone x-100, and 0.1% β-mercaptoethanol. pH7.3). The lysate was centrifuged at a speed of 12000 rpm and temperature of 4°C for 20 minutes. The supernatant was transferred in to a fresh 50 mL tube containing 3 mL 50% v/v GST-agarose beads (Sigma) suspended in the binding buffer (10mM Tris, 150 mM NaCl, and 0.1% β-mercaptoethanol. pH7.3) and then incubated at 4°C for 2 hours. The beads that bound to fusion protein were washed two times with the binding buffer for 15 minutes each time and then subjected to elution buffer (50 mM Tris, 20 mM reduced Glutathione, pH 8). Beads were gently centrifuged and the supernatant was transferred to a fresh tube where its concentration was determined. The beads were washed and stored as instructed by the manufacturer. Protein concentration was measured using the Bradford assay (Bio-Rad). Protein solution was aliquoted

and stored at -80° C. All steps of protein expression and purification were analyzed using SDS-Poly acrylamide gel electrophoresis (SDS-PAGE).

2.5 *para*-Nitrophenyl Phosphate Assay

The synthetic substrate, para-nitrophenyl-phosphate di(tris) salt (pNPP), was purchased from (Sigma-Aldrich), dissolved in MiliQ-water in a concentration of 200 mM, aliquoted and promptly stored at - 20°C. The reaction buffer (TBS) was prepared at a 5X-concentration and added to the 96-well plate (Sarstedt) at final concentrations of (50mM Tris, 50mM Bis-tris, 150 mM NaCl, and 5.0 mM DTT). The substrate solution was warmed up at 30°C for 10 minutes and then reaction was initiated by adding protein solutions of GST-hYVH1, GST-cleaved hYVH1, hYVH1 mutants or VHR dual specific protein tyrosine phosphatase (Biomol). Volume of reaction was 100 μL. All assays were performed in triplicates including blanks in which reaction mixture does not contain enzyme in order to measure the spontaneous hydrolysis of the substrate. The reaction was left to proceed at 30°C for 15 minutes and then 150 μL of stopping reaction solution (0.33 M NaOH.) was added. The assay plate was left for 5 minutes and then read at 405 nm by a spectrophotometer (Ultra Microplate Reader – Bio-TEK Instruments, Inc). The concentration of the product was determined by measuring the intensity pNP yellow colour at 405 nm and using Beer's Law ($A_\lambda = \epsilon\ C\ L$), where A is the absorbance of sample subtracted from blank, ϵ is the molar extinction coefficient which is $1.78 \times 10^4\ M^{-1}\ cm^{-1}$ for pNPP, C is the concentration of product, and L is the path length which is 0.71 cm when the final volume of reaction mixture is 250 μL in 96-well plate (SARSTEDT).

22

2.6 [3-*ortho*-Methylfluorescein Phosphate] Assay

Synthetic phosphatase substrate, 3-O-methylfluorescein phosphate (OMFP), was purchased from Sigma and solutions were freshly-prepared for each run. OMFP was dissolved in dimethyl sulfoxide (DMSO) at a concentration of 12.5 mM, vortexed, sonicated, and then used as a stock solution to prepare assay substrate solutions. The reaction buffer used was 50mM.Tris, 50mM.Bis-tris and 150mM.NaCl (TBS); this mixture covers a pH range from 4 to 9. The pH of the buffer was controlled as needed for the assay using NaOH or HCl. Assays were performed in a reducing environment using 5mM dithiothreitol (DTT).

To confirm hYVH1 phosphatase activity one substrate concentration was subjected to serial concentration of wild type hYVH1 and one concentration of hYVH1-C115S mutants. Using excitation/emission (485/535 nm) intensity of RFUs was measured continuously for 15 minutes after adding the enzyme to substrate solution in TBS buffer.pH 6.

To determine kinetic parameters, substrate working solutions pH 4, 5, 6, 7, 8, and 9 (4 different pH values per assay) were loaded onto a Nunc 96-well plate (Sigma-Aldrich) at a volume of 250 μL in serial concentrations of 5, 10, 20, 40, 80, 100, 150, 200, 400, 600, 900, 1200 μM (final concentration). DMSO percentage was maintained at a concentration of 1%. Blanks for these concentrations were included in the assay by loading reaction buffer instead of enzyme solution to measure the spontaneous hydrolysis rate. The 96-well plate was

23

pre-warmed 10 minutes at 30°C. Enzyme solution was then added to the assay promptly at a final concentration of 1 μM.

OMF production was continuously measured, using excitation/emission (485/535 nm), for one hour. Raw data output by the spectrofluorometer were reorganized, using Microsoft Office-Excel, into columns that represent RFUs verses time individually for each substrate concentration. Intensity of non-enzymatic spontaneous hydrolysis was subtracted. RFUs were converted into micromoles of product using a standard curve for OMF. This standard curve was performed by measuring the intensity of fluorescence (RFUs) of serial concentrations of OMF in the reaction buffer used for OMFP assays; data of RFUs values were plotted against the corresponding data of OMF concentrations and then used to convert RFUs into concentration units.

Slopes of the production rate (picomoles per seconds) were plotted versus concentration of substrate solutions within the first twenty minutes and taken as initial velocities of reaction (V_0), and then fitted to Michaelis-Menton Expression: ($V_0 = V\text{max}[S]/(S+K_m)$). Where S is the value of substrate concentration, Vmax is maximum velocity, which does not increase due to increasing the substrate concentration; and the K_m is the concentration of substrate in which the enzyme reaches half of its V_{max}. k_{cat} then calculated using equation(2): ($k_{cat} = V_{max} / [E]_T$). Where E is the value of total enzyme concentration by moles in the reaction mixture.

24

2.7 [6, 8-di-Fluoro-4-Methylumbelliferyl Phosphate] Assay

DiFMUP was purchased from (Invitrogen) and dissolved in DMSO with final concentration of 126.3 mM. Substrate solution at this concentration was aliquoted and stored in -20°C to be used as the stock solution. Reaction buffer used was TBS at the same concentrations of the OMFP assays including DMSO and DTT. The phosphatase activity was confirmed using comparison assay between serial concentrations of wild type hYVH1 along with C115S mutant in one concentration of DiFMUP.

To determinatine kinetic parameters serial substrate working solutions were loaded onto the 96-well plate at a volume of 100 μL in serial concentrations of 25, 50, 150, 300, 400, 500, 600, 900, 1200, 2400 μM (final concentration). The 96-well plate was pre-warmed for 10 minutes at 30°C. Enzyme solution of hYVH1, wild type or mutants, was promptly added to the assay mixture in final concentration of 0.6 μM. Blanks were included in the assay by loading the same serial substrate concentrations with reaction buffer instead of enzyme solution.

Excitation of production, DiFMU, was performed using wavelength 355 nm and its fluorescence was measured at 465 nm. As mentioned previously, the fluorescence intensity was continuously measured for one hour, reorganized as RFUs versus substrate concentration, blanks were subtracted, and then RFUs were converted into units of concentrations using standard curves of DiFMU.

Conversion of the data of RFUs into units of moles was processed using standard solutions that were prepared from precisely known serial concentrations of products (DiFMU). These serial concentrations were performed for each pH from 4 to 9 separately.

Signal of fluorescence was then measured using specific excitation/emission wavelengths. Data of products fluorescence verses concentrations for each pH were plotted to prepare standard curves. Using (Microsoft Soft Office-Excel 2003), standard curves were presented as equations with which data of RFUs of enzymatic assays can be converted into their equivalent units of moles. RFUs finally graphed as slops of curves that show initial velocities of reaction verses serial concentration of substrate (V_0). Kinetic parameters, K_{cat} & K_m, were determined and plotted together in relation of k_{cat}/K_m value verses pH value, with which the effect of pH on enzyme kinetic activity will be presented.

2.8 Cell Culture and Transfection

Human embryonic kidney 293 *(HEK 293)* cells were grown at 37°C in DMEM/F-12 media with 10% fetal bovine serum, 1% L-glutamine, and 1% penicillin/streptomycin in 10 cm plates. Cells were subcultured every two/three days once they reached 80-90% confluency. $1.5*10^6$ cells were split one day before transfection. Cells were transfected with wild type hYVH1 or C115 hYVH1 cDNA inserted in Flag-tagged *CMV* expression vector *(pCMV)*. Transfection was performed using FuGene 12 μL, 4μg of DNA, and 200μL of serum-free media were mixed together, incubated for 20 min and then added to the cells.

2.9 Cell Lysis and Immunoprecipitation

Transfected 293-HEK cells were lysed after being washed with cold phosphate buffered saline (PBS) and placed on ice. The cells were lysed in 1mL of

26

lysis buffer consisting of 50 mM Tris-HCl pH 7.4, 1% Triton X-100 detergent, 150mM NaCl, 0.1% SDS, and protease inhibitors. The lysates were then spun down at 15000 rpm for 20 min and the pellet was discarded. While spinning, the Anti-Flag M2-agarose affinity resin was washed twice with immunoprecipitation (IP) wash buffer (50 mM Tris-HCl, 0.1% Triton X-100 detergent, 150mM NaCl, and 0.1% SDS. pH 7.4). 20μL of the beads were diluted to 100μL with the IP wash buffer and used to immunoprecipitate 300μL of the cellular lysate for 2 h. The beads were then gently washed three times with ice-cold IP wash buffer and two times with ice-cold assay reaction buffer (Tris.50 mM, Bis-tris.50mM, NaCl.150mM, and 5 mM DTT. pH 6). To analyze the efficiency of transfection and immunoprecipitation, 35μL of 2x SDS-PAGE loading buffer was added to the bead pellet, which were recovered after the assay, and analyzed on SDS-PAGE.

2.10 OMFP and DiFMUP *In vivo* Assays

250 μL of OMFP (600μM) or 100 μL of DiFMUP (900 μM) solution in the assay reaction buffer (50 mM.Tris, 50mM.Bis-tris, 150mM.NaCl, and 5 mM DTT. pH 6) was added to the beads in 1.5 mL-microcentrifuge tube with one sample as a blank. Samples were incubated for one hour at 30°C with continuous gentle shaking. Samples were spun down and the supernatant was transferred quantitatively into the 96-well plate and scanned using spectrofluorometer.

2.11 GST Cleavage assay

Protein was expressed in BLR-*E.coli* and purified as mentioned above and stored at -80°C until the day of cleavage assay. Immobilized thrombin on agarose

(Sigma-Aldrich) was used to cleave GST-hYVH1. Cleavage assay was performed in a batch format. Solution of purified GST-hYVH1 was dialyzed and exchanged into ice-cold cleavage assay buffer (50mM.Tris-HCl pH 8, 10 mM. $CaCl_2$). Protein was subjected to dialysis with cleavage assay buffer using 20 mL for four times to ensure complete removal of elution buffer contents. The protein concentration was measured prior proceeding to cleavage assay. 1 mL of 50% v/v thrombin-agarose resin was added to protein solution in final concentration of 1 mg/mL in total volume 10 mL. The reaction mixture was incubated at 4°C for three hours. Reaction was stopped by spinning down the resin and transferring the supernatant into fresh 15 mL Falcon-tube. Protein was stored at -80°C and the resin was washed and stored at 8-2°C in a storage buffer as instructed by the manufacturer. The protein solution that recovered from cleavage assay was applied to GST-sepharose resin at 4°C for 2 hours and then spun down. Supernatant was transferred into fresh tube, and then reconcentrated using (Centricon) and then aliquoted and stored at -80°C.

CHAPTER 3

RESULTS

3.1 Expression and Purification of Recombinant hYVH1:

In order to acquire ample amounts of pure recombinant hYVH1 to be used in kinetic analysis, hYVH1 was over expressed as a GST fusion protein in BLR-*E.coli* cells. BLR cells were transformed with *pGEX.4T1* vector encoding an N-terminal-GST tagged hYVH1. After inoculation in *Luria-Bertani* (LB) at 37°C to a density of 0.6 (600 nm), protein expression was induced by the addition of IPTG (0.8 mM) and incubation at room temperature with shaking speed of 250 rpm. Harvested cells were lysed by sonication and then spun down at 11000 rpm for 25 min. Supernatant was loaded on to 3 mL of 50% (v/v) GST-sepharose resin. After 2 hours incubation for binding followed by washing twice, bound protein was eluted using 20 mM of reduced glutathione dissolved in Tris-buffered solution. However, the amount of protein yielded per 500 mL was low and did not exceed 1.4 mg. Although, GST-hYVH1 was soluble and quite pure using this protocol (Fig. 4), optimization was necessary to increase the yield.

To increase the yield of protein expressed, culture was grown in 2XYT formula, which is more enriched media than the regular LB media, and subjected to the same procedure of expression and purification. This substitution of media resulted in an increase of up to 3 mg of protein per 500 mL of culture. By adding 1.0% sterile glycerol to the 2XYT and increasing the optical density of the cultures up to 1.5-2.0 (600 nm), protein yield was dramatically increased by ~ 9-fold (Fig. 5).

29
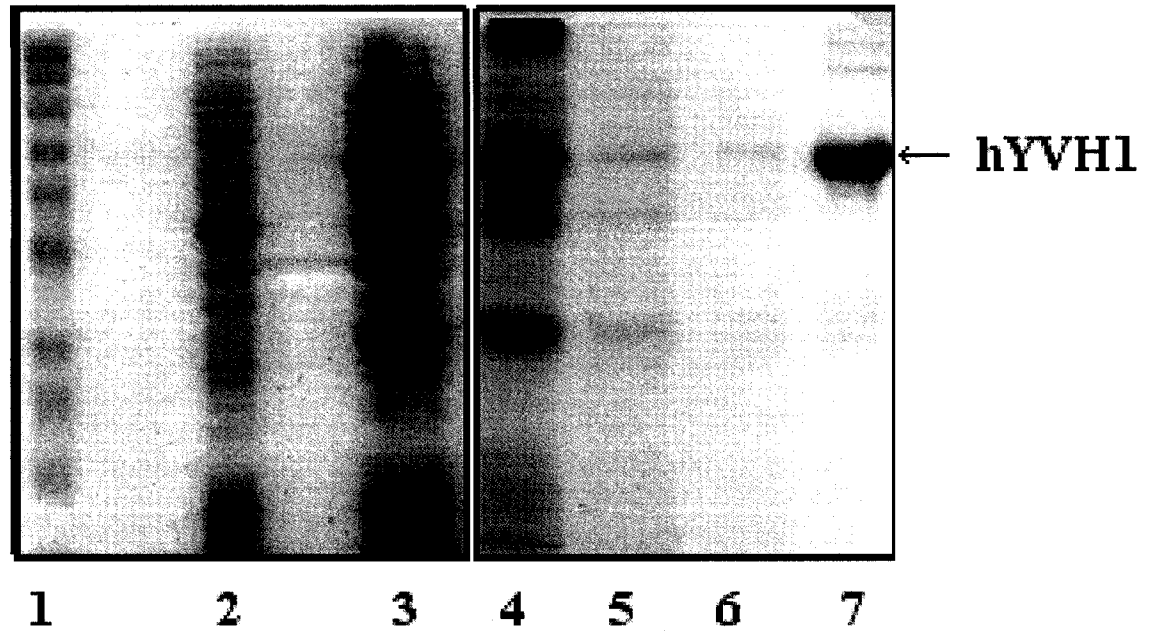
Figure 4: Expression and purification of recombinant GST-tagged hYVH1.

The lanes from 1 to 7 represent steps of protein expression and purification as the following:

Lane 1, protein ladder. Lane 2, uninduced crude lysate. Lane 3, induced crude lysate. Lane 4, aliquot was taken from the supernatant of sonicated-lysate after centrifugation in 12000 rpm at 4°C for 25 min. Lane 5, 6, first and second washes of the resin. Lane 7, band of GST-hYVH1.

30

These results demonstrated that hYVH1 can be highly expressed and purified using the GST-fusion approach, yielding suitable protein amounts for enzymatic studies.

3.2 Is hYVH1 Poor *para*-Nitrophenyl Phosphatase:

The preliminary efforts to measure the catalytic activity of purified hYVH1 were accomplished using *para*-nitrophenylphosphate (pNPP), which is the most common synthetic substrate used to assay protein tyrosine phosphatases activity *in vitro*. pNPP structurally mimics phospho-tyrosine and is initially colorless. Phosphatases hydrolyze the phosphate moiety to produce *para*-nitrophenol and inorganic phosphate. *para*-nitrophenol is also colorless, but once it is deprotonated by the adding of NaOH into the reaction mixture it becomes yellow-colored and can be quantitatively measured. The intensity of the yellow color is directly proportional to the concentration of nitrophenol (Fig. 6). The yellow colour was measured spectrophotometrically at 405 nm and the concentration was evaluated using Beer's Law.

Unexpectedly, hYVH1 showed extremely low activity against pNPP even after increasing the molarity of protein in the assay up to 2.62 μM, and the substrate concentration up to 50 mM. Furthermore, a wide range of buffers and environmental settings were implemented but all failed to detect the activity levels typical for PTP enzymes.

A well-characterized dual-specific protein tyrosine phosphatase, VHR, was used as a positive control. VHR showed a specific activity of 7233 ($\pm$150) picomoles min^{-1} μg^{-1} while the highest specific activity that can be detected for

31
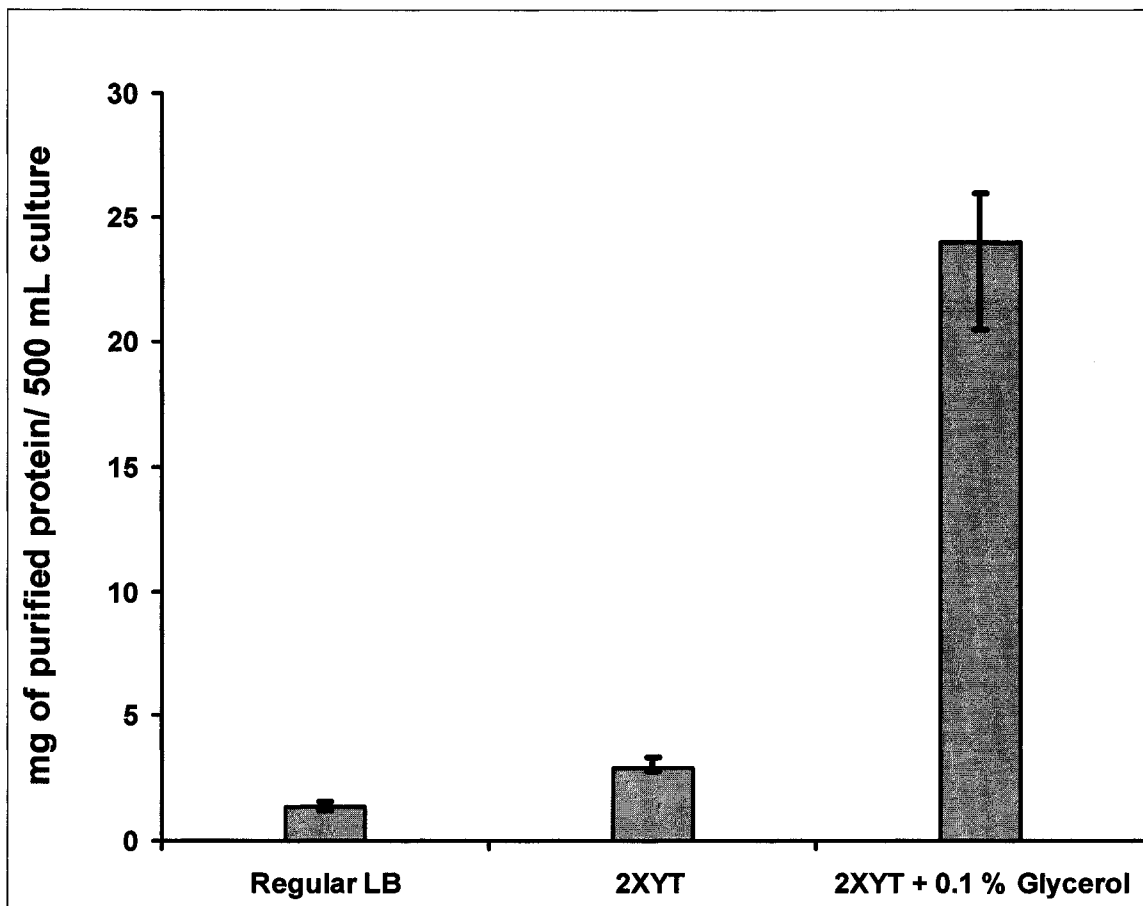
Figure 5: Optimization of GST-hYVH1 expression in E.coli.

The first column from the left shows the yield of protein expressed in the conventional LB. The second column shows the yield after using the enriched media, 2XYT. The third column shows the effect of adding 1% glycerol in to the 2XYT media.
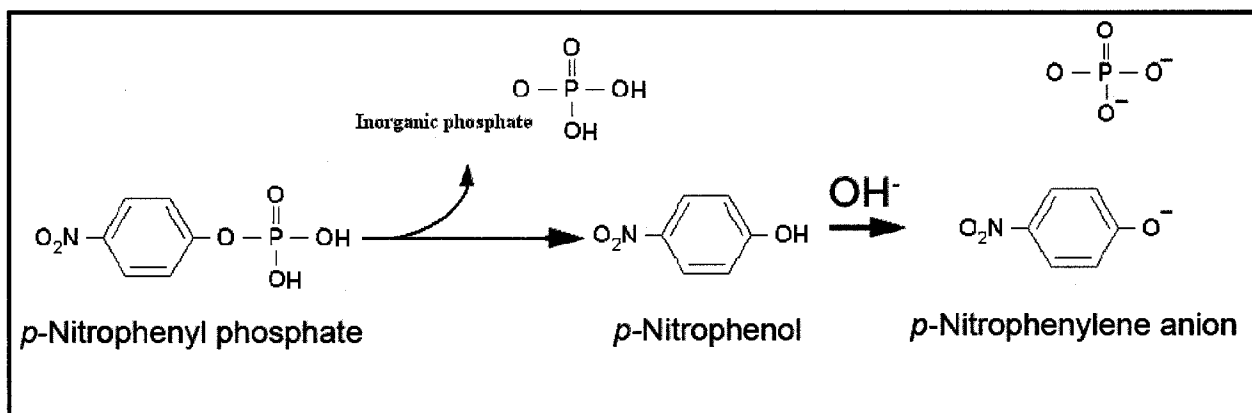
Figure 6: pNPP assay principle. pNPP is initially colorless. Phosphatases hydrolyze pNPP to *para*-nitrophenol and inorganic phosphate. *para*-Nitrophenol has to be deprotonated by adding NaOH to be colored and can be spectrophotometrically measured at 405 nm.

33

hYVH1 was 2.13 (±0.18) picomoles min^{-1} μg^{-1} which is ~3390-fold lower than the VHR activity (Fig. 7). These results revealed the intrinsically low *in vitro* phosphatase activity of recombinant hYVH1, also that pNPP can not serve as a viable substrate to study the enzymatic properties of hYVH1.

3.3 Detection of Phosphatase Activity towards OMFP:

Since pNPP is a poor substrate for studying hYVH1, a more sensitive assay based on the fluorescence properties of 3-O-methylfluorescein phosphate (OMFP) was used (Fig. 8).

To determine whether hYVH1 possesses a phosphatase activity towards OMFP, serial amounts of wild type (2.0, 5.0, 10.0, 13.5, and 17.0 μg) and C115S (17.0 μg) were added to 500 μM of OMFP solution in TBS buffer pH 7., 10). Phosphatase activity of hYVH1 towards OMFP was detected and was proportional to its concentration in the reaction mixture; while C115S showed no activity even after increasing the concentration of protein up to (17.0 μg) (Fig. 9). Data of RFUs were converted using the standard curve for the product, OMF (Fig. 10). The specif- ic activity of hYVH1 towards OMFP was 5.0 $X10^3$ (± 1.0) picomoles min^{-1} μg^{-1}.

To determine Kinetic parameters k_{cat} and K_m, 1.0 μM of hYVH1 was added to serial concentrations of OMFP in TBS pH 7. Initial velocities of OMF production was measured in all concentrations, plotted in a graph versus concentrations of substrate, and then fitted with Michealis Menton equation (Fig. 11). K_m was determined as the concentration of substrate when the enzyme reaches half of its maximum velocity (V_{max}). The turnover number *(k_{cat})* was determined using the following equation:

34
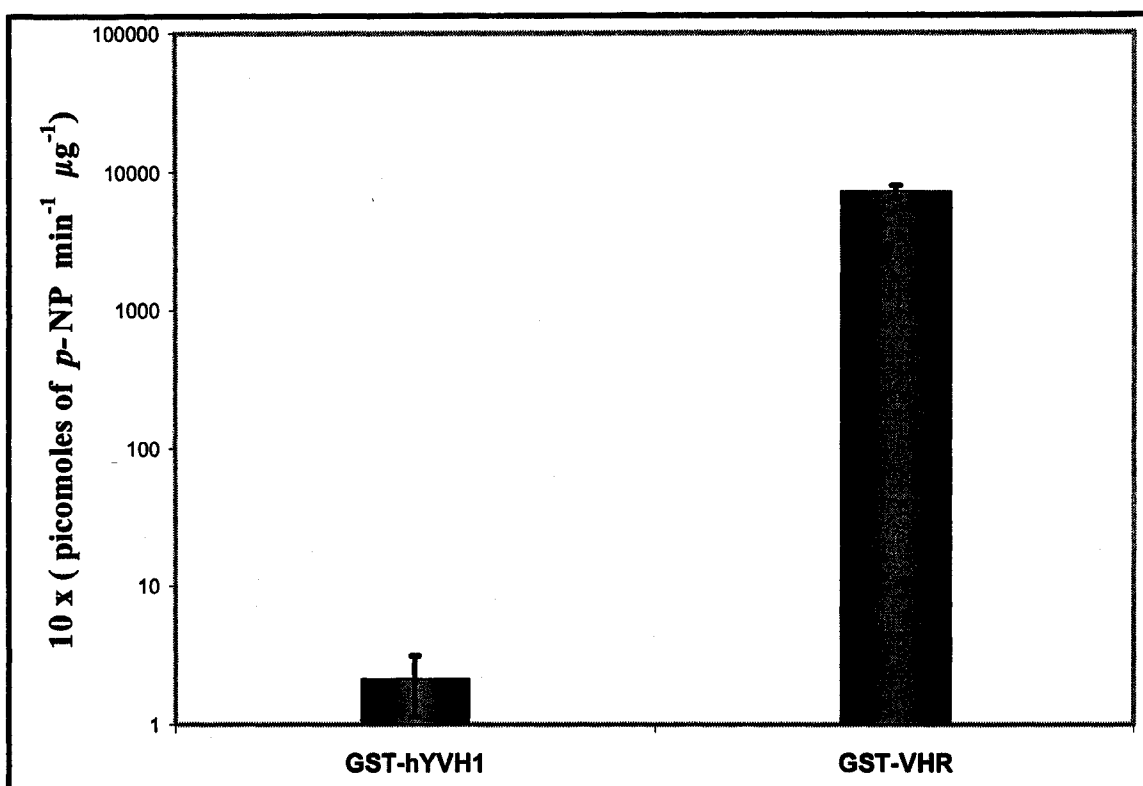
Figure 7: Comparison between specific activities of GST-VHR and GST-hYVH1.

Numbers are multiplied by 10 to make them presentable by the logarithmic scale. The regular scale cannot be used due to the very low specific activity of GST-hYVH1.

35

CH$_3$O $\qquad$ O $\qquad$ OPO$_3{}^{2-}$

O

O
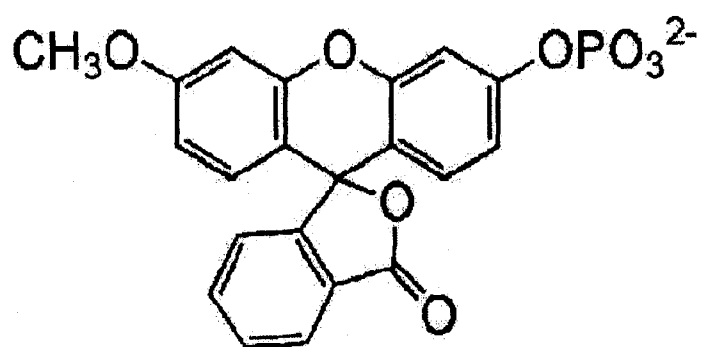
OMFP

Figure 8: Structural formula of 3-O-methylfluorescein phosphate (OMFP).

The synthetic substrate, OMFP, is widely used to detect phosphatase activity. Although the multiple-ringed structure makes it more reactive with protein tyrosine phosphatase, it has several shortcomings as a substrate for studying enzymes in different pH values.

36
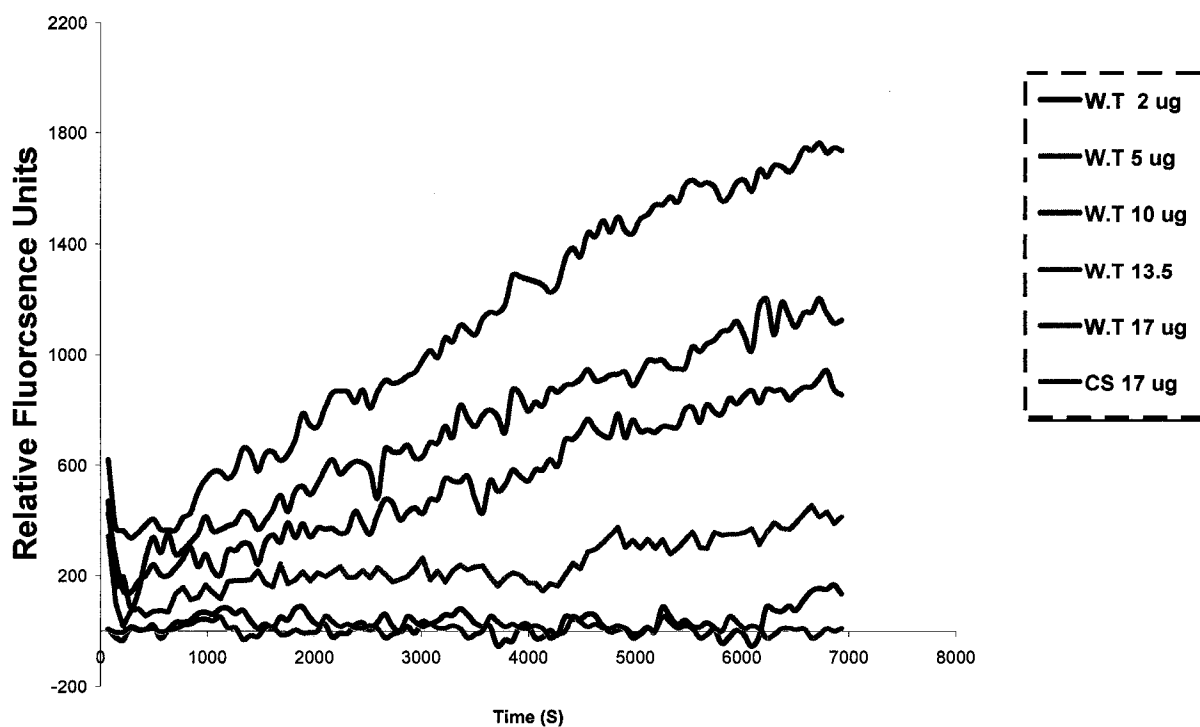
Figure. 9: Phosphatase activity of hYVH1. Serial concentrations of enzyme were added to the substrate solution in a fluorescence plate. Intensity of fluorescence was measured. The graph shows the increase in the intensity is directly proportional to the increase in the enzyme concentration. The red curve shows the absence of phosphatase activity in hYVH1 C115S mutant confirming that the activity t of wild type hYVH1 is indeed phosphatase activity.

37

The standard curve plots Relative Fluorescence Units (y-axis, 0 to 7000) versus μM of OMF (x-axis, 0 to 25).

Inset box:
pH 7
$y = 253.62x + 62.987$
$R^2 = 0.9995$

Figure 10: The standard curve of OMF. Phosphatase activity hydrolyses the OMFP producing OMF and PO4. Serial concentrations of OMF were precisely prepared and scanned by the fluorometer. RFUs then plotted in the graph versus corresponding concentrations. This standard curve and its equation were used to convert RFUs data, that given by fluorometer in phosphatase assays, into concentration units, micromoles.

38

($k_{cat} = V_{max}/[E]_T$). k_{cat} for hYVH1 towards OMFP was determined to be 5.4x10^{-4} s^{-1} ($\pm$ 0.2X10^{-4}), and K_m is 250 μM ($\pm$ 30).

These results confirmed that recombinant hYVH1 does possess intrinsic phosphatase activity towards OMFP, and kinetic parameters can be determined. However, OMFP has a high rate of spontaneous hydroly- sis especially in the ranger of pH 7 or ghreater. In addition, it has a poor solubility in aqueous solutions especially in pH valu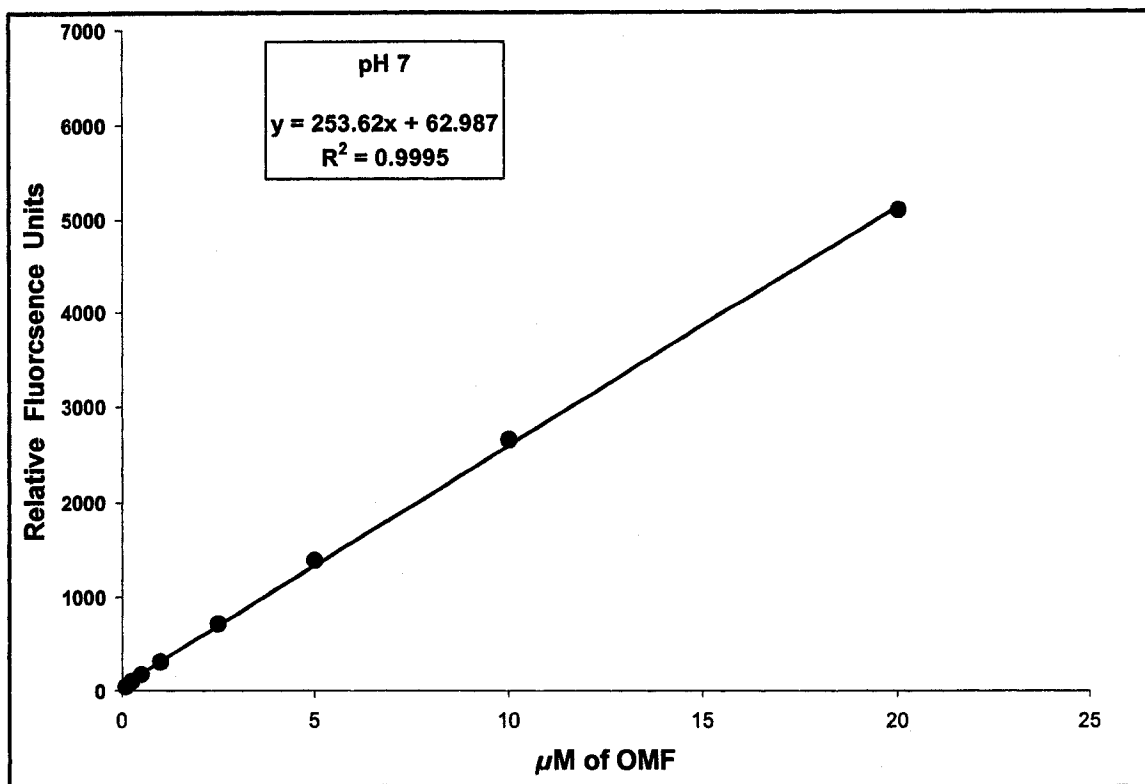es $\leq$ 6. These physical/chemical properties of OMFP made using it to study the effect of pH variation on phosphatase activity of hYVH1 impractical.

3.4 DiFMUP Is an Ideal Model to Study hYVH1 Phosphatase Activity:

The synthetic substrate, 6,8-difluoro-4-methyl-umbelliferyl phosphate (DIFMUP) is a recently introduced as a substrate that possesses intrinsic physical and chemical properties that make it a suitable substrate to study the kinetics of phosphatases (Fig. 12). Phosphatase activity of hYVH1 towards DiFMUP was confirmed using VHR as a positive control along with hYVH1- C115S as a negative control. Wild type hYVH1, C115S and VHR were added in amounts of 0.01, 0.01 and 0.001 mg respectively to a 900 μM of DiIFMUP solution in 100 μL TBS buffer pH6 and 5 mM DTT using 96-well fluorescence plates. Reaction mixtures were incubated for 20 minutes at 30°C. RFUs were converted to products concentrations using standard curve for the product, DiFMU (Fig. 13). Specific activity for each protein was calculated as micromoles of product divided by time units (minutes) and mass units (micrograms) of protein.

No activity was detected for C115S confirming that the hydrolysis of substrate is

39
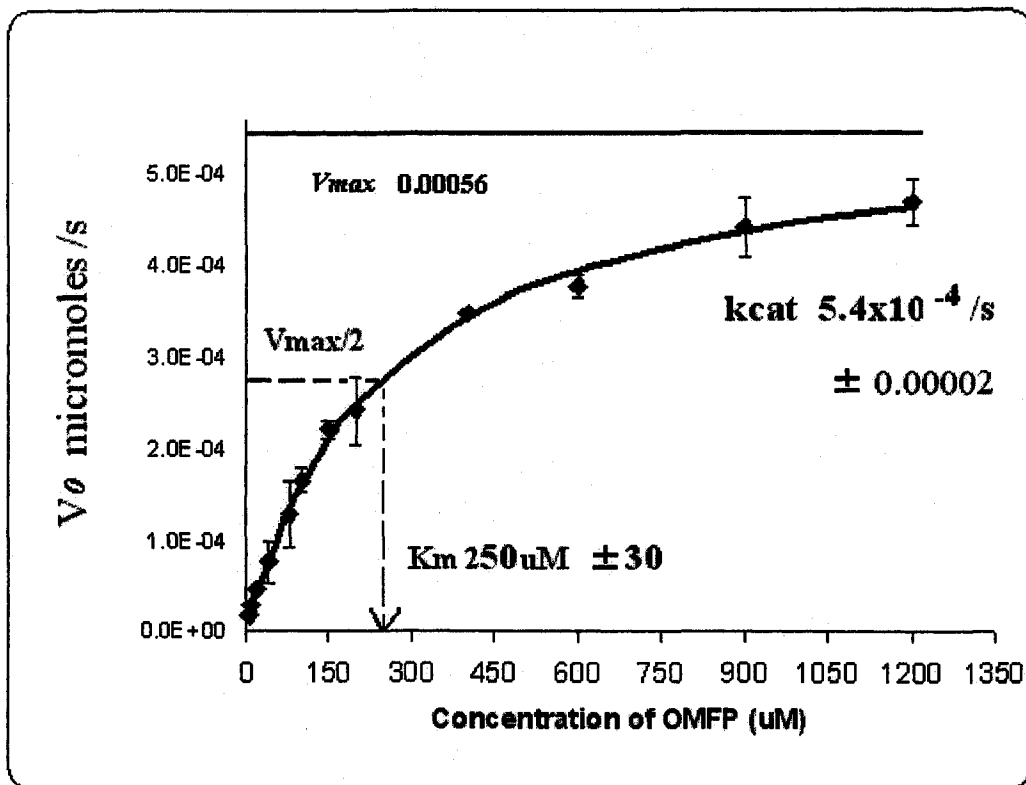
Figure 11: Determination of K_m and k_{cat} of hYVH1 towards OMFP.

Serial concentrations of OMFP solution in TBS buffer pH 6 were subjected to a constant concentration of hYVH1 at temperature of 30°C. Initial velocities of hYVH1 in these concentrations were measure and plotted as seen in the graph. K_m was determined as it is the concentration of substrate that corresponding to the half value of the maximum velocity. k_{cat} was calculated using Michaelis-Menten Equation The graph shows velocity in the level of hundreds of picomoles per second while K_m value is at the level of micromoles.

40
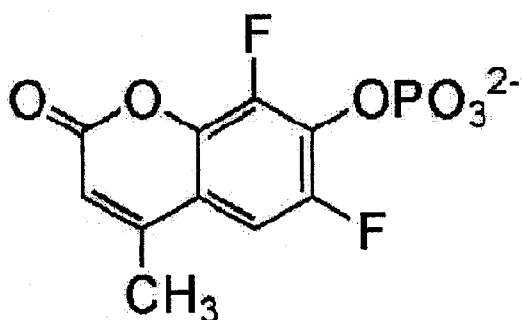
DiFMUP

Figure.12: 6,8-difluoro-4-methyl-umbelliferyl phosphate (DiFMUP):

The synthetic molecule DiFMUP was recently introduced as a phosphatase substrate, its

reactivity and stability have made it an ideal model that can be used to study low active

phosphatases in a wide range of pH variations.

41

phosphatase activity. Wild type hYVH1 specific activity was 5.5×10^3 picomoles min^{-1} μg^{-1} ($\pm$ 1400) while specific activity of VHR was 2.4×10^6 picomoles min^{-1} μg^{-1}($\pm$15000) ($\pm$15000); in other words, hYVH1 has shown ~ 436-fold less activity than VHR against DiFMUP (Fig. 14).

Kinetic parameters were determined by measuring initial velocities of serial concentrations of substrate solution in TBS buffer with 5 mM DTT and pH 6. Assays were conducted at temperature of 30°C. V_{max} of hYVH1 towards DiFMUP was determined to be 3.2×10^{-3} μM/s ($\pm$ 0.000025) and consequently k_{cat} was calculated to be 5.5×10^{-3} s^{-1} ($\pm$ 0.4$\times$10^{-3}). K_m was 520 μM ($\pm$ 25) (Fig. 15). DiFMUP characteristically showed a low rate of spontaneous hydrolysis, along with high signal of emitting fluorescence. With these stability and sensitivity properties, mechanistic studies on hYVH1 could be done further.

3.5 hYVH1 Obeys The Catalytic Mechanism of Protein Tyrosine Phosphates:

The PTP superfamily is characterised by a catalytic mechanism that includes general acid/base catalysis. This stage of catalysis makes kinetic parameters of PTP pH-dependent. Therefore, studying kinetics of hYVH1 in different pH values will reveal whether it possesses general acid/base catalysis. Using a continuous fluorescence assay, kinetic parameters of hYVH1 were determined in pH a range from 4 to 9. Serial concentrations of substrate solutions were prepared in the assay buffer and then loaded onto the fluorescence plate. The enzyme was added to the wells at a concentration of 0.6 μM. Plates were scanned to measure RFUs which in turn were converted to

42

Top chart legend: ☷ pH7 ◆ pH8 ▲ pH9

pH8
y = 945.99x - 67.672
R^2 = 0.997

pH7
y = 890.67x - 313.28
R^2 = 0.991

pH9
y = 944.79x + 315.77
R^2 = 0.998

Y-axis: Relative Fluorscence Units
X-axis: Concentration of DiFMU (µM)

Bottom chart legend: ● pH4 ▲ pH5 ☷ pH6

pH 6
y = 1120.6x - 421.75
R^2 = 0.9971

pH 5
y = 640.96x - 358.32
R^2 = 0.9949

pH4
y = 301.12x - 248.99
R^2 = 0.9759

Y-axis: Relative Fluorscence Units
X-axis: Concentration of DiFMU (µM)

43
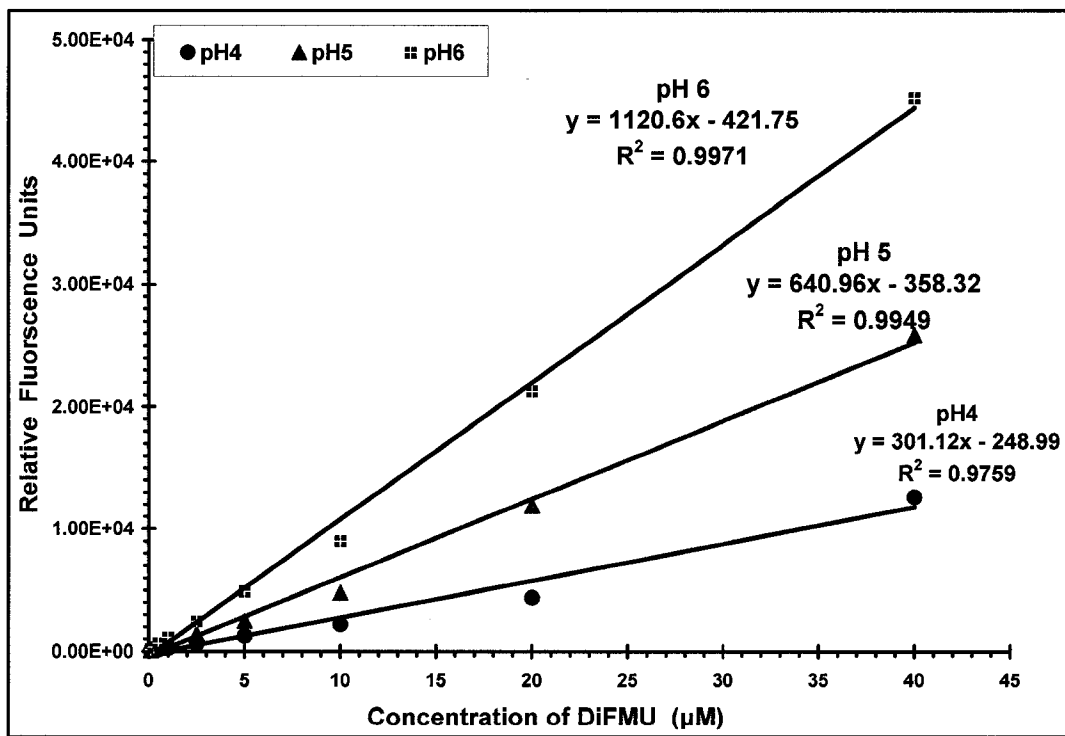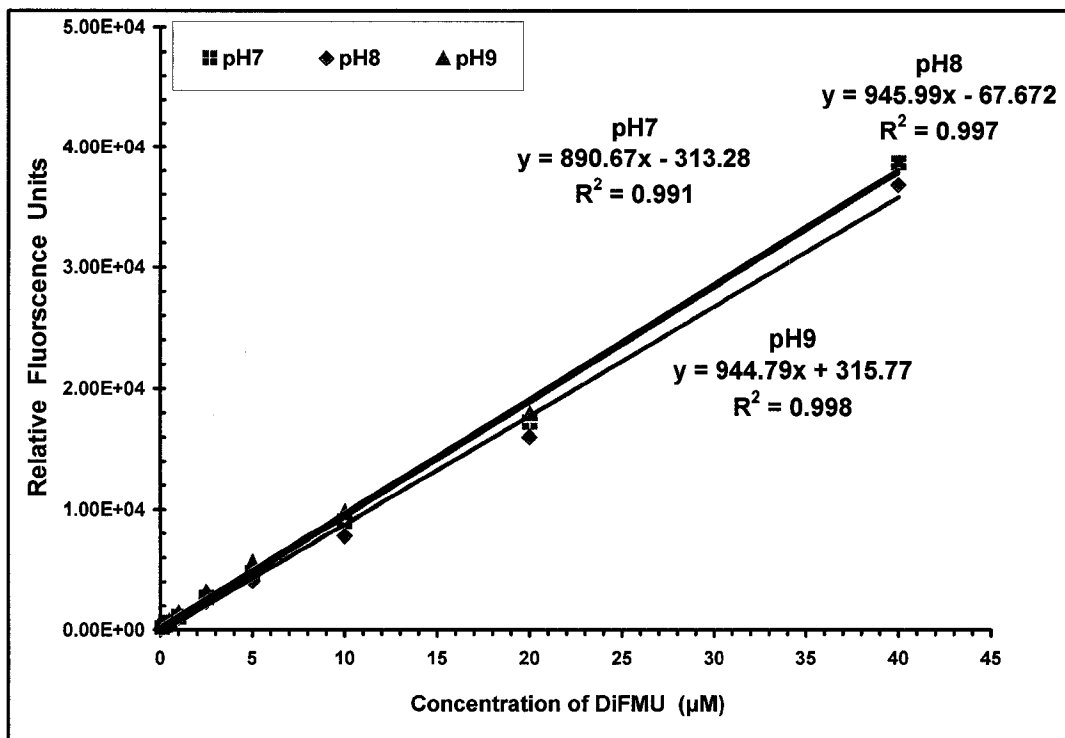
Figure. 13. The Standard curves of DiFMU.

6,8-difluoro-4-methyl-umbelliferyl phosphate (DiFMU) is the product of phosphatase activity toward DiFMUP. Serial concentrations for DIFMU in the reaction buffer (TBS) were precisely prepared and loaded onto fluorescence plate in the same volume of reaction of phosphatase assays. This was done for pH range from 4 to 9. Plate was scanned and data of RFUs were blotted versus the corresponding concentrations. As presented in the graph, standard cureves and their equation were performed using Microsoft Office Excel. These standard curves were used to convert RFUs into units of concentration.

44
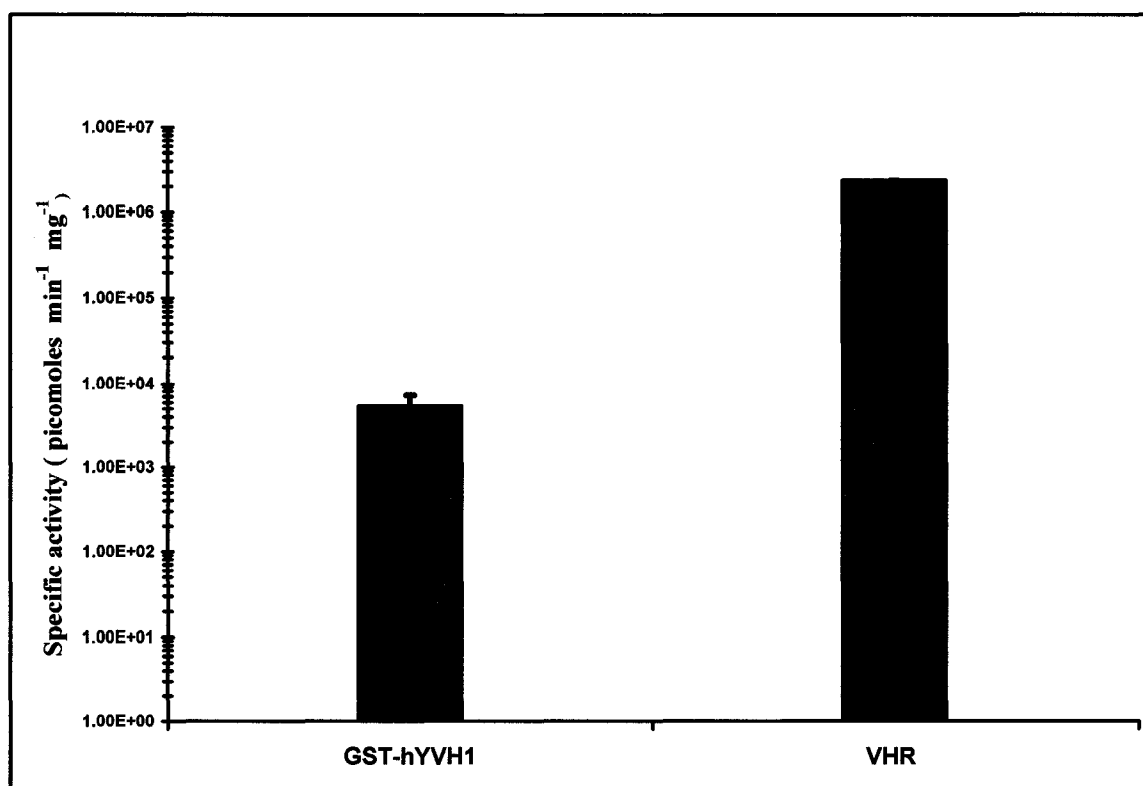
Figure 14: Specific activity of hYVH1 and VHR towards DiFMUP. Protein (wild type, C115S, or VHR) was added to 0.9 mM of DiFMUP solution in TBS buffer pH 6. Assay was run at temperature of 30°C. RFUs were converted into micromoles using standard curves. Specific activity of hYVH1 was measured to be 5.5 X10^3 (± 1400) picomoles min^{-1} µg^{-1} whereas VHR's is 24 X10^5 (± 15000) picomole min^{-1} µg^{-1}, which means approximate 436-fold difference. The graph was set on the logarithmic scale due to the vast variation between specific activities of both proteins.

45
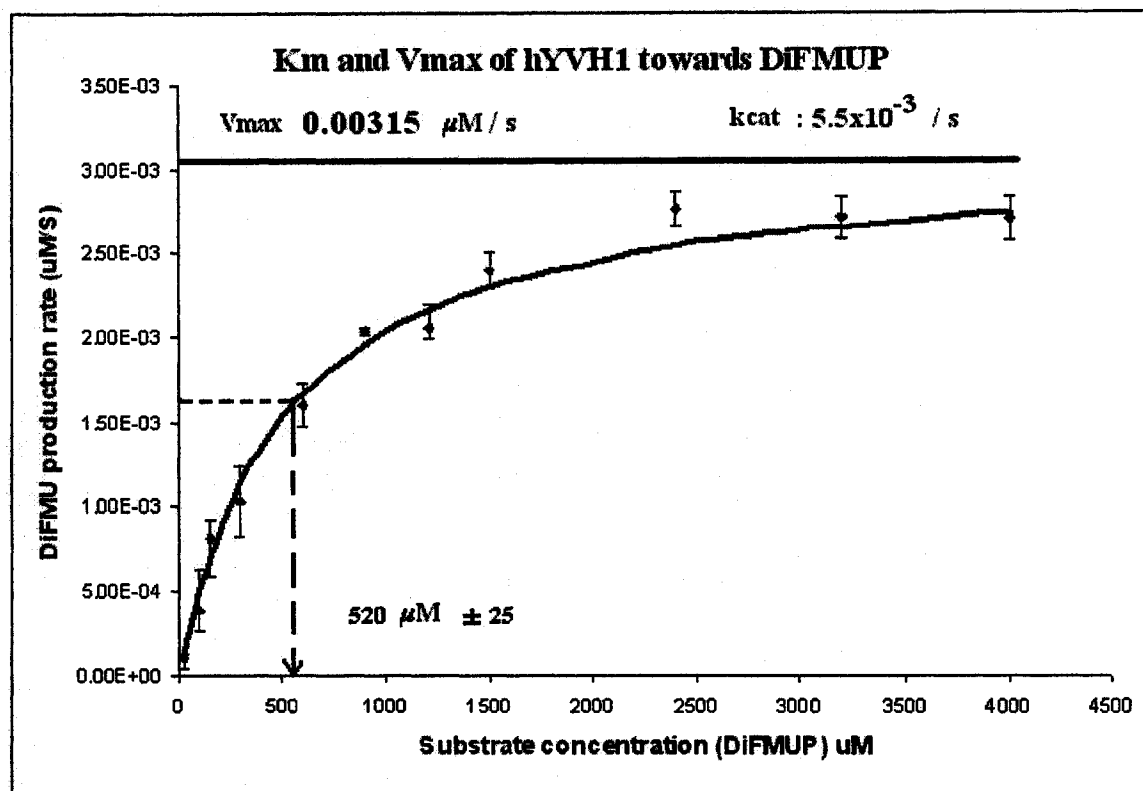
Figure 15: K_m and V_{max} of hYVH1 towards DiFMUP. Serial concentrations of DiFMUP solution were subjected to 0.6 μM of hYVH1 in TBS buffer. pH 6 and temperature of 30°C. K_m of hYVH1 was plotted as the concentration of substrate when the velocity reaches half of its maximum value. RFUs were converted into units of concentration using standard curves of DIFMU. K_m was measure to be 520 μM ($\pm$ 25) and k_{cat} was 3.15 X 10^{-3} μM S^{-1}.

46

micromoles. V_{max} and k_{cat} of protein at each pH value were determined and plotted as k_{cat}/K_m values versus pH values; in addition to k_{cat} values versus pH values (Fig 16, 17).

Although, these results showed a significantly low K_{cat} value for hYVH1 and consequently low value of k_{cat}/K_m compared to other members of PTP superfamily, they showed a significant pH dependency, indicating that it employs acid/base catalysis within its catalytic mechanism that is typical for most PTPs superfamily members (Fig 2).

3.6 Identification of a Novel Critical Residue for Acid/base Catalysis in hYVH1

Many DUS PTPs have been shown to have their catalytic acid/base located 31 residues upstream of the catalytic Cys. In the hYVH1, that position is held by Asp84. Therefore, to identify the catalytic acid/base residue, three proximate aspartates, D74, D84, and D89, were mutated separately using PCR-based site directed mutagenesis, and then the phosphatase activity for the three mutants, D84A, D89A, and D74A were assayed.

Proteins were expressed and then purified using the above mentioned protocol that was developed for the wild type. Equal amounts of Wild type hYVH1, D74A, D84A, D89A hYVH1 were added to 1 mM of DIFMUP solution in TBS as a preliminary assay was conducted to observe the effect of any of these mutations on the activity of hYVH1. Specific activities of the proteins, wild type, D74A, D84A, and D89A

47

were 5.5 X10^3 (± 0.18), 4.8 X10^3 (± 0.09), 0.27 X10^3 (± 0.04), and 0.38 X10^3 (±0.005) picomoles min^{-1}μg^{-1} respectively (Fig. 18).

These results showed that mutation of D74 did not effect the activity of hYVH1 whereas mutations in D84 or D89 substantially decreased the specific activity of hYVH1 towards the DiFMUP. Therefore, further investigations were needed to identify which residue is the catalytic acid/base. Since hYVH1 displayed pH dependency toward DiFMUP hydrolysis, measuring kinetics parameters of the mutant forms of the enzyme in various pH values may reveal what role each residue plays in the catalytic mechanism.

Using continuous fluorescence assay, kinetic parameters of hYVH1-D84A and hYVH1-D89A in a range of pH values from 4 to 9 were determined. Fig. 19 shows the pH profiles of k_{cat}/K_m for both mutants along with the pH profile of k_{cat}/K_m for wild type hYVH1. Interestingly, hYVH1-D84A was apparently pH-independent and showed much less activity than did the wild type. The D89A mutant also showed decrease in activity, although slightly higher than the D84A mutant at most of the pH values. The exception was in the lowest pH value (pH 4), at which the activity of D89A mutant was approximately equal to the activity of the wild type. These results suggest that the catalytic acid/base residue is Asp84 while Asp89 likely plays a critical role in stabilizing the catalytic acid/base.

3.7 OMFP and DiFMUP *In vivo* Assays:

hYVH1 is an eukaryotic enzyme and needs to be studied as it is expressed in eukaryotic cellular environment, which is highly different from bacterial cellular environment.

48
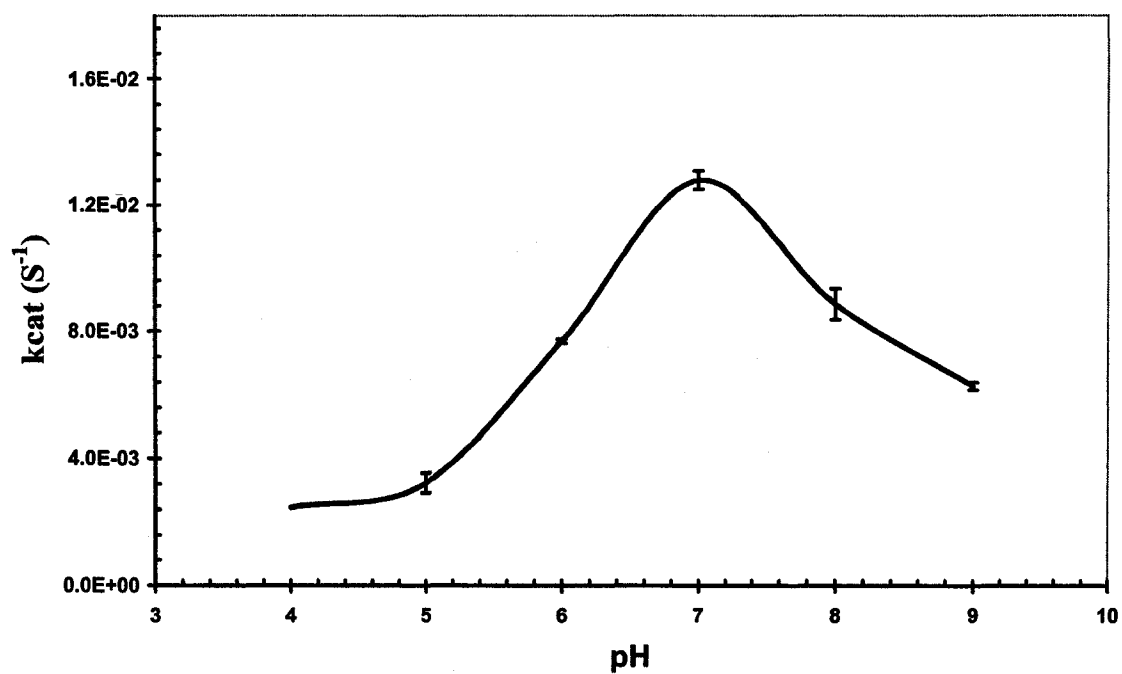
Figure 16: Effect of pH on *kcat* of hYVH1. *kcat* was calculated with dividing V_{max} (

μM/s) by concentration of enzyme (μM). The bell-shaped graph shows that it is pH-dependent revealing the presence of general acid/base catalysis. The optimum pH for

hYVH1 is pH 7.

49
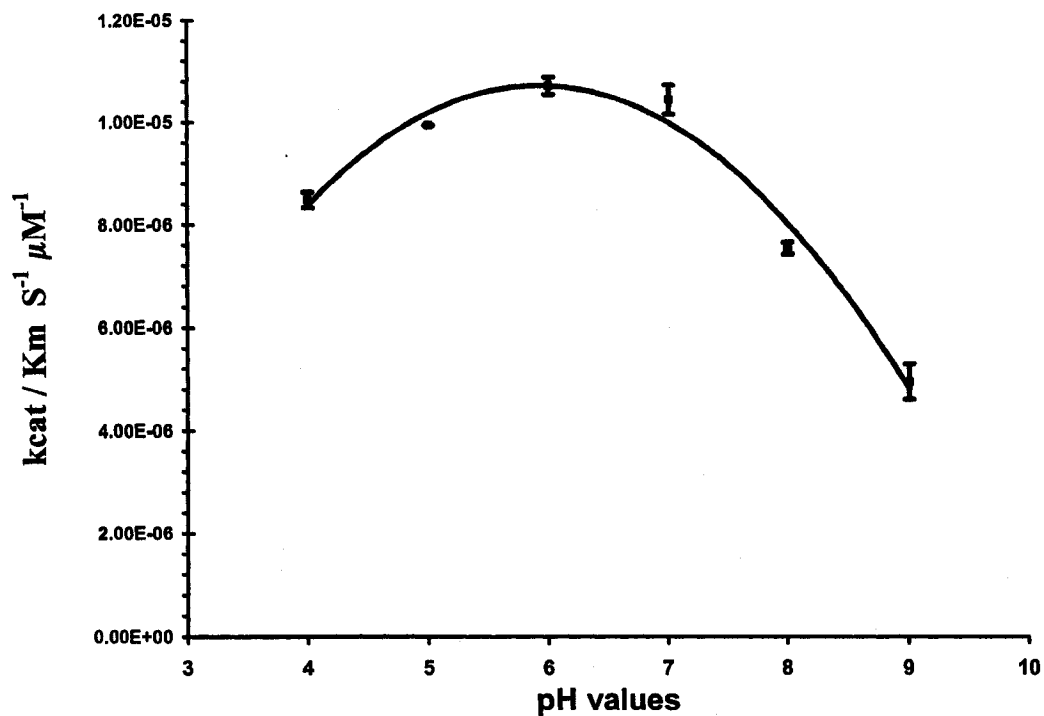
Figure 17: pH profile of k_{cat}/K_m for wild type hYVH1.

Kinetic parameters (k_{cat} and K_m) of wild type hYVH1 in pH values (4, 5, 6, 7, 8, and 9) were determined and plotted as a pH values versus k_{cat}/K_m. The bell-shaped curve demonstrates the pH-dependency of kinetic parameters of hYVH1, and proving that hYVH1 is following the catalytic mechanism of PTP superfamily which include general acid/base catalysis.

50
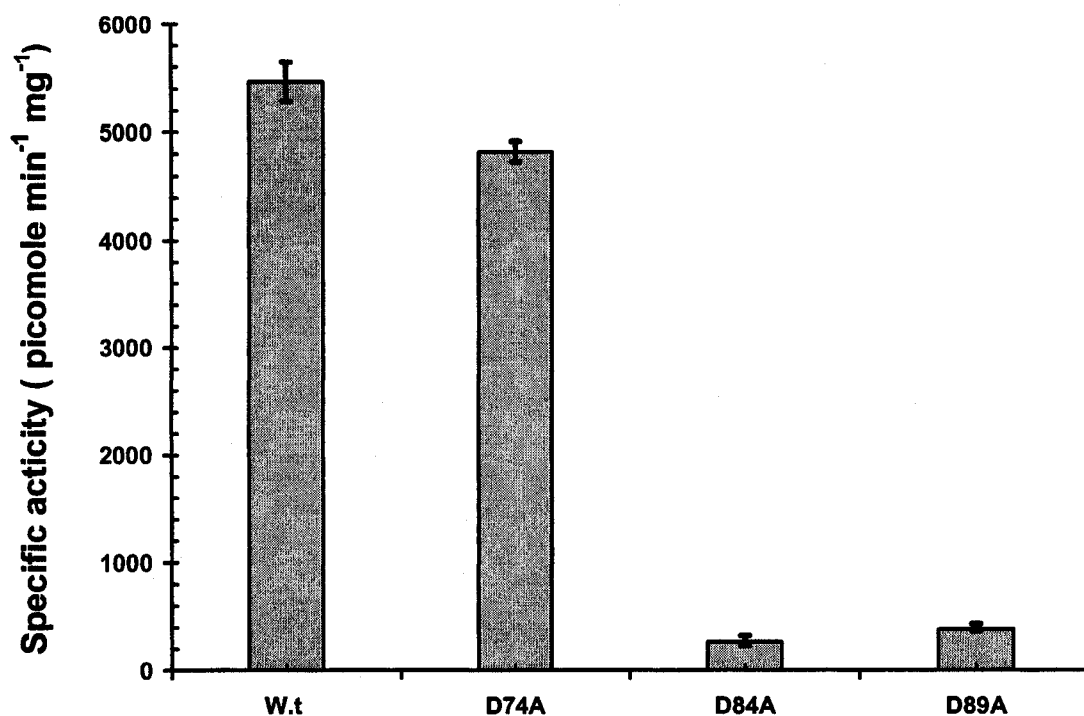
Figure 18: The effect of mutations in D74, D84, and D89 on phosphatase activity of hYVH1 towards DiFMUP. The D74A mutant did not lose significant specific activity compared to wild type. However, D84A and D89A mutant forms were drastically inactivated suggesting that both residues play essential roles in the catalytic mechanism of hYVH1.

51
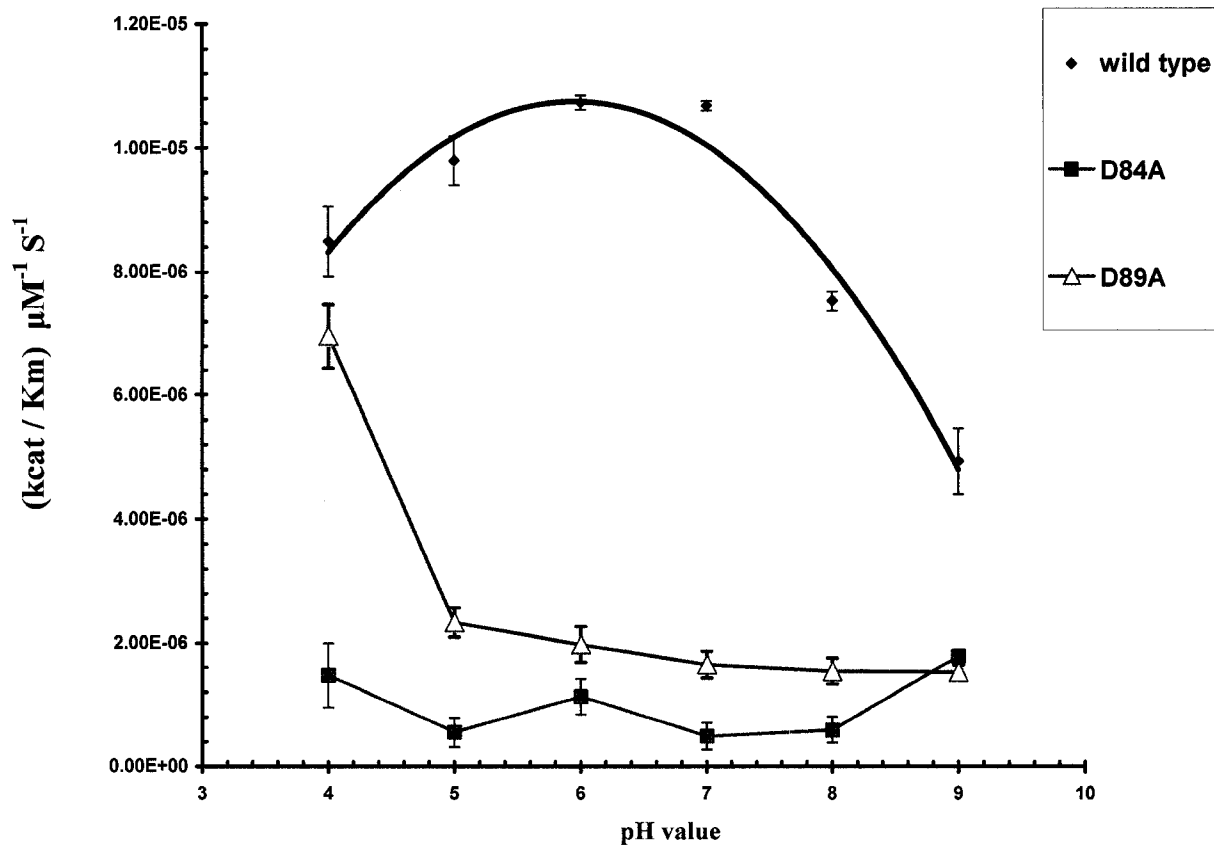
Figure 19: Comparison of pH values versus kinetic parameters of wild type hYVH1, D84A and D89A mutant forms. The red graph shows that the D84A mutant low activity is pH-independent over the range of pH values from 4 to 9. The blue graph shows the pH profile of kinetic parameters for the D89A mutant form, which is also low as the D84A mutant form with some pH dependency in the acidic range. The activity of D89A mutant form at pH4 is almost equal to activity of wild type hYVH1.

52

In the *in vivo* assays, wild type hYVH1 or C115S was transiently transfected into HEK-293 cells using recombinant cDNA of hYVH1 wild type or C115S that inserted into a pCMV FLAG-tagged expression vector.

The harvested cells were lysed and then immuno-precipitated using anti-Flag M2-agarose affinity resin. Bound resin was washed 3 times using IP washing buffer and 2 times with assay reaction buffer, TBS, to ensure the removal of non-specific proteins bound to the resin. Assays were run by loading substrate solution of OMFP or DiFMUP into resin and incubated at 30°C for one hour.

Readings of blank and untransfected cells were subtracted from reading of samples that contain lysates of transfected cells. RFUs were converted into units of moles using equations of standard curves. Equal amounts of the beads recovered from the assay were loaded onto SDS-PAGE (Fig. 20). hYVH1 wild type showed activity against OMFP and DiFMUP while C115S variant was inactive (Fig. 21).

These semi-*in vivo* assays were established so they can be used in the future for studying hYVH1 expressed in mammalian cells. Using these assays hYVH1 can be studied in different circumstances that may regulate its activity such as post-translational modifications or protein-protein interactions.

3.8 Cleavage of GST Tag:

A deeper understanding of the enzymatic properties of hYVH1 can be achieved by studying its mechanistic structure. For these studies to be done in

Reproduced with permission of the copyright owner. Further reproduction prohibited without permission.

collaboration with Dr. Brain Crane at Cornell University an untagged version of hYVH1 is needed. Wild type GST-tagged hYVH1 was subjected to thrombin cleavage procedure using an agarose immobilized-thrombin (Fig. 22). As a control, a sample of GST-tagged hYVH1 was aliquoted immediately before adding the thrombin and was subjected to all steps of the cleavage assay but without exposing it to the thrombin.

This sample was aliquoted to get preliminary information on the stability of hYVH1 from this multi steps procedure, and to check it for any loss of activity. As shown in (Fig. 23), no activity loss was detected suggesting that the catalytic integrity will be preserved during our sample preparation for structure studies.
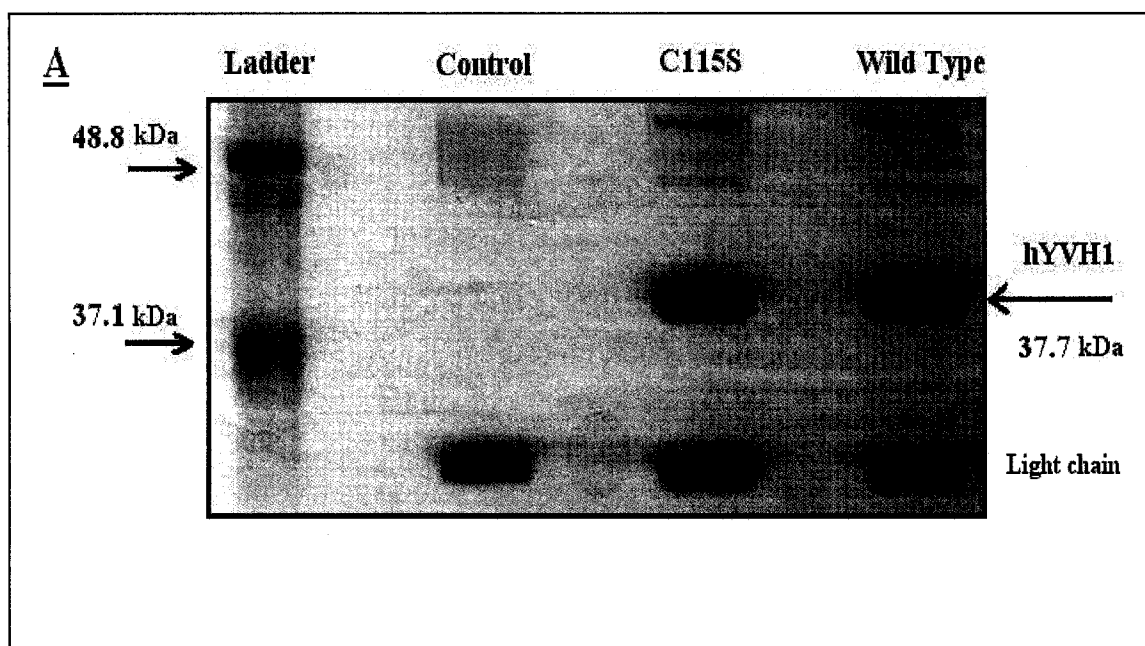
Figure 20. Expression of hYVH1 in 293-HEK cells.

A representative gel showing levels of hYVH1 varients in 293 cells. Lane 1: the molecular weight standards. Lane 2: the untransfected control sample. Lane 3: the C115S mutant sample. Lane 4: the wild type hYVH1 sample.

55
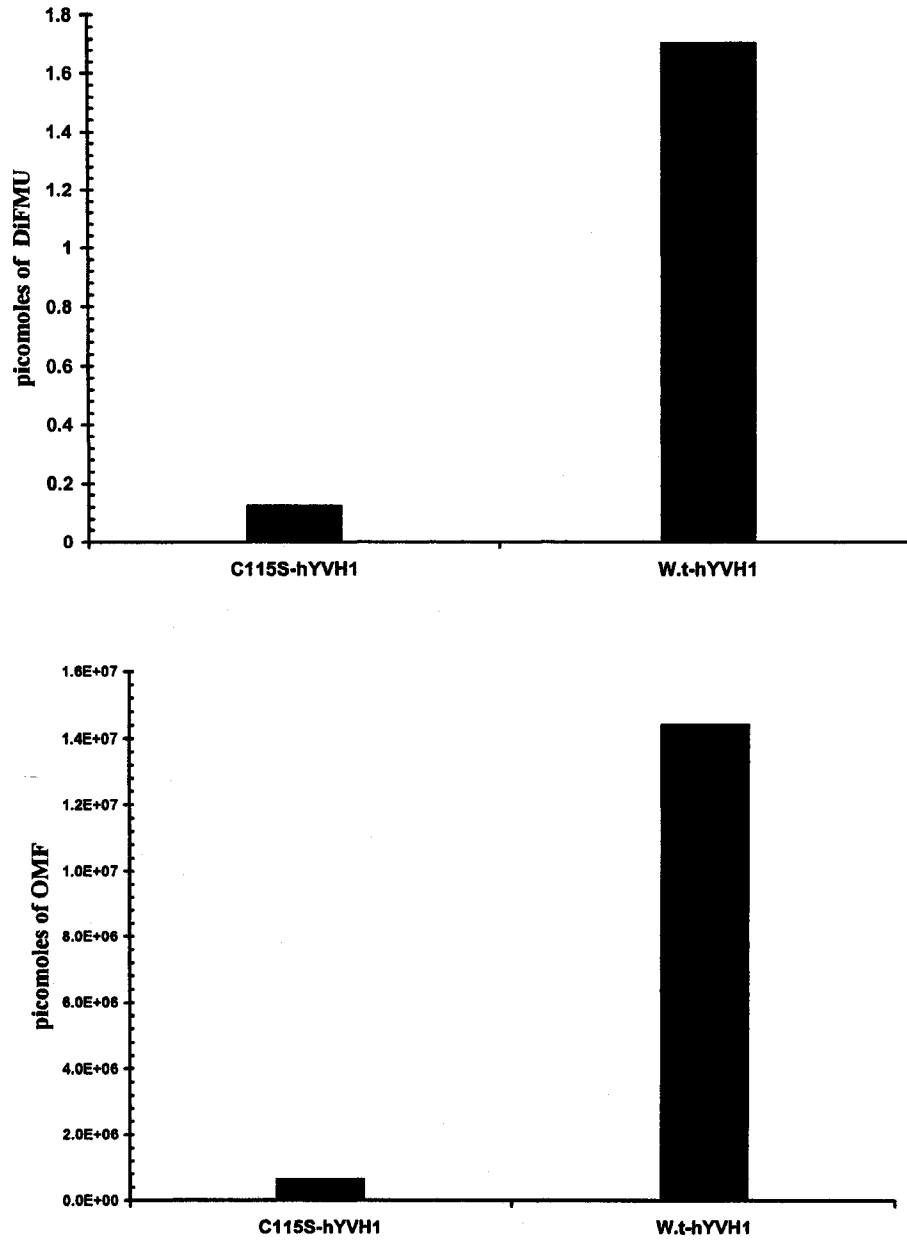
Figure 21: Detection of hYVH1 activity that expressed in mammalian cells.

The upper graph shows the OMFP activity of wild type hYVH1 compared to hYVH1 C115S mutant. The lower graph shows the DiFMUP activity of wild type compared to C115S mutant.

56
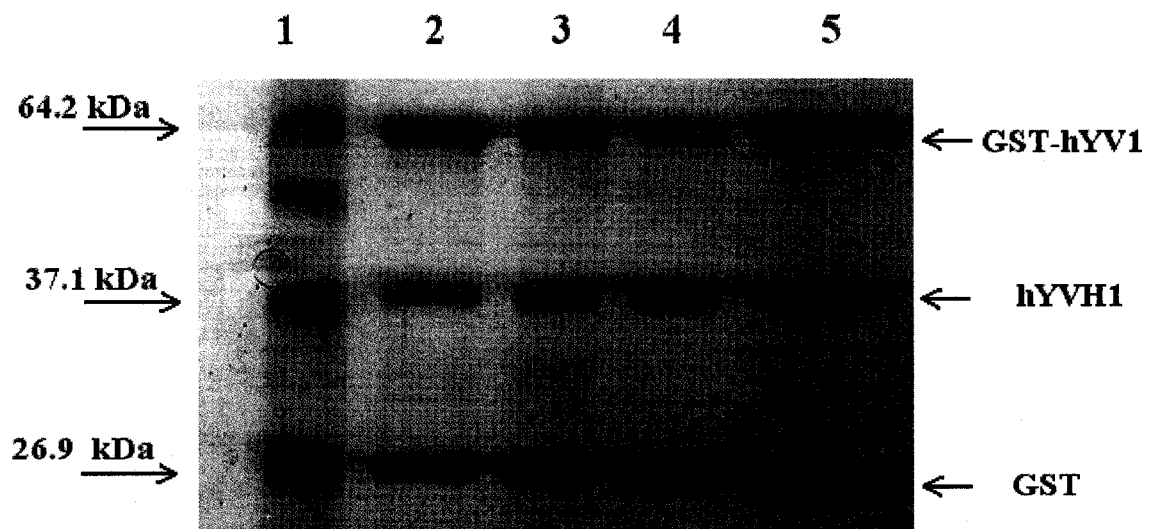
Figure 22. Cleavage of GST tag. The lanes show aliquots taken from the reaction mixture as following: Lane1: the molecular weight standards. Lane 2: the first hour. Lane 3: the second hour, Lane 4: the third hour. Lane 5: the fourth hour.

57
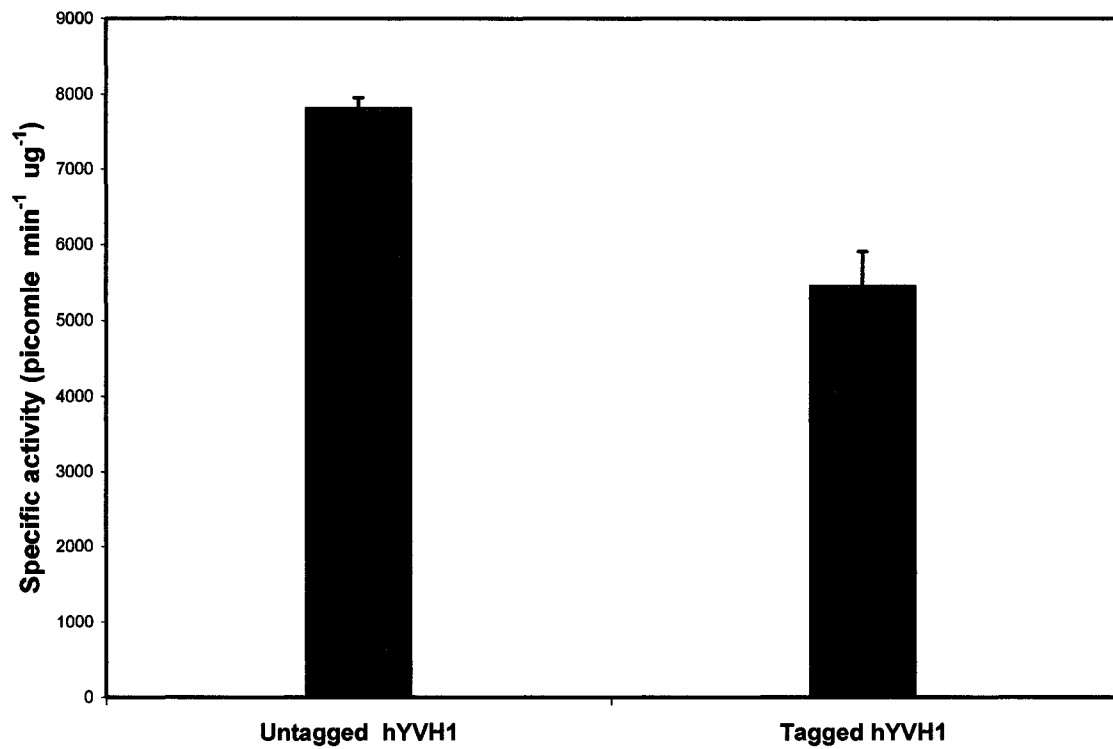
Figure.23: Specific activity of untagged hYVH1 compared to specific activity of GST-tagged hYVH1

58

CHAPTER 4

DISCUSSION

The dual specificity protein tyrosine phosphatase hYVH1 (DUS PTP hYVH1) is an enzyme that was identified in 1999 and found to be highly expressed in human tissues (56). Its gene maps to chromosome Iq-21-q23, which is observed to be amplified in human liposarcomas (57, 58,59). Its orthologue in yeast was shown to play a role in cellular growth, sporulation, and glycogen accumulation (51-53). This role is predicted to be highly conserved since hYVH1 is able to compensate the role of YVH1 in the yeast cells (56).

Notably, information about the physiological role, substrate and regulation of hYVH1 is lacking since 1999. In this study we aimed to establish reproducible *in vivo* and *in vitro* phosphatase assays that can be used in the future for studying hYVH1 under different conditions. These assays were used in this study to characterize the catalytic properties of this dual specificity protein phosphatase. Finally, purification of untagged hYVH1 was undertaken for the purpose of future structural studies.

4.1 Optimizing A Purification Large Scale-Protocol for Recombinant hYVH1that Expressed in Bacterial Cells

Using the conventional media (LB media) bacteria cultures yielded small amounts of protein. Also, using 2XYT, which is a more enriched media, only

59

slightly increased the protein yield. This could be explained by the low density of bacterial cells that can be reached using these formulas without effecting the cells integrity. However, the addition of 1% (v/v) glycerol into 2XYT media, and increasing the OD 600 target of the culture dramatically increased the yield to amounts that was enough to perform multiple enzymatic assays. This is important since it attained amounts of enzyme solution that purified from the same batch. Also, large quantities of protein were needed to cover full pH profile assays, cleavage assay, and preparation for X-ray crystallography study.

4.2 Detection of hYVH1 Phosphatase Activity

The most common synthetic phosphatase substrate that has been used over the past decade is para-nitrophenyl phosphate (pNPP). Since hYVH1 belongs to PTP superfamily; in our study pNPP is of particular interest because of its similarity with the tyrosine. A wide range of buffers that are usually used in protein phosphatase assays along with many environmental settings were examined. The well-characterized dual specificity phosphatase VHR was used as a positive control. However, hYVH1 showed extremely low activity against pNPP leading us to look for a more suitable way to detect phosphatase activity of hYVH1.

There were certain synthetic phosphatase substrates that may increase the sensitivity of detecting the apparent low activity of our enzyme of interest, fluorescence substrates such as 3-O-methylfluorescein phosphate (OMFP) or 6,8-difluoro-4-methyl-umbelliferyl phosphate (DiFMU) were widely used to probe phosphatase activity.

60

hYVH1 activity against OMFP was detectable and quantifiable. This enzymatic activity was confirmed using the C115S mutant form, which was completely inactive indicating that the hydrolysis measured for the wild type hYVH1 is indeed specific. The rate of hydrolysis was measurable and directly proportional to the concentration of the enzyme in the reaction mixture.

hYVH1 showed a specific activity towards OMFP of 5.0 $\times 10^3$ picomole min^{-1} μg^{-1} ($\pm$ 1.0) which is approximate 2350-fold higher than pNPP. With this activity the kinetic parameters of hYVH1 could be measured. k_{cat} was determined to be 0.54 $\times 10^{-3}$ (s^{-1}) and Km was 250 μM. Comparing to other members of PTP superfamily listed on Tables 1 and 2.

hYVH1 displayed a very low turn over number (k_{cat}) but Km was within the range of other highly active phosphatase such as PTP1. At this point, experiments proceeded to measure the kinetic parameters in different pH values to reveal whether acid/base catalysis is present. However, OMFP showed poor solubility an pH values less than 7, and extremely poor stability in pH values higher than 7. Therefore, results of the pH profile of hYVH1 towards OMFP were inconclusive. Specific activity of hYVH1 against DiFMUP was determined to be 5.5 x 10^3 picomoles min^{-1} μg^{-1}. This activity is almost equivalent to its activity with OMFP. Kinetic parameters of hYVH1 with DiFMUP also were measured as k_{cat}: 5.5 x10^{-3} ($\pm$ 0.04 x10^{-3}) (s^{-1}) and K_m: 520 uM ($\pm$25).

61

4.3 Detection of acid base catalysis

Certain shortcomings of the physical and chemical properties of OMFP precluded it from being a viable model for studying hYVH1 behaviour at different pH values. On the other hand, DIFMUP showed high solubility with a good stability over all the pH values used in the assays, in addition to the high fluorescence signal. Kinetic constants (k_{cat} and K_m) of hYVH1 against DiFMUP were measured, k_{cat}/K_m were calculated and then plotted as a function of pH value. Both the k_{cat} and K_{cat}/K_m showed a bell-shaped curve demonstrating pH dependency with a slope of +1 on the acidic side and slope of -2 on the basic side (Fig. 17). The bell-shaped pH profile of k_{cat}/K_m or k_{cat} revealed that the catalysis is governed by the ionization states of the catalytic residues, the catalytic cysteine (Cys115), or the general acid/base.

Alignment of the primary sequence of hYVH1 with other DUS PTPs showed that there are three adjacent Asp residues Asp74, Asp84, Asp89 (Fig. 24). The alignment tells that both D84 and D89 are invariant but not the D74. The preliminary step was to explore the effect of altering these residues on the hYVH1 phosphatase activity. Mutations were performed using PCR-site directed mutagenesis. Proteins were expressed and purified using the same protocol and then subjected to phosphatase assay against DiFMUP along with wild type hYVH1 (Fig. 18).

62

Table.1. The kinetic parameters for different members of PTPs superfamily towards OMFP.

	K_m (mM)	k_{cat} (S^{-1})	K_{cat}/K_m (mM^{-1} S^{-1})
Cdc14 (59)	1.0	3.4	3.4
PRL-1 (60)	0.022	0.19 X10^{-3}	8.6 X10^{-3}
PTP1 (61)	0.2	2.6	13
MKP3 (62)	0.096	18.0 X10^{-3}	0.190 X10^{-3}
VHR (61)	0.1	1.5	15
hYVH1	0.25	0.54X10^{-3}	2.16 X10^{-3}

Table.2. The kinetic parameters for different members of PTPs superfamily towards DiFMUP.

	K_m (mM)	k_{cat} (S^{-1})	K_{cat}/K_m (S^{-1} mM^{-1})
Cdc14 (59)	0.01	8.1	810
PRL-1 (60)	0.0046	0.143 X10^{-3}	0.031 X10^{-3}
MKP3 (63)	0.017	3.5 X10^{-3}	0.206
MKP4 (63)	0.011	0.16 X10^{-3}	14.5 X10^{-3}
MKP5 (63)	0.08	0.15	1.9
VHR (63)	0.045	0.21	4.7
hYVH1	0.52	5.5 X10^{-3}	10.6 X10^{-3}

63

```
                  ↓     ⌄
MKP-1―219  QYKSIPVEDNHKADISSWFNEAIDFIDSIKNAGGR-VFVHCQAGISRSATICLAYLMR1
MKP-2―241  QYKCIPVEDNHKADISSWFMEAIEYIDAVKDCRGR-VLVHCQAGISRSATICLAYLMMI
MKP-3―254  KYKQIPISDHWSQNLSQFFPEAISFIDEARGKNCG-VLVHCLAGISRSVTVTVAYLMQI
MKP-4―251  HYKQIPISDHWSQNLSRFFPEAIEFIDEALSQNCG-VLVHCLAGVSRSVTVTVAYLMQI
MKP-5―369  NYKRLPATDSNKQNLRQYFEEAFEFIEEAHQCQKG-LLIHCQAGVSRSATIVIAYLMKI
MKP-8―112  RYLGVEAHDSPAFDMSIHFQTAADFIHRALSQPGGKILVHCAVGVSRSATLVLAYLML1
hYVH1― 76  WRLFVPALDKPETDLLSHLDRCVAFIGQARAEGRA-VLVHCHAGVSRSVAIITAFLMK1
            :     *      ::      :   .   :*          :::** .*:***.::  *:**
```

Figure 24: An alignment for 6 members of MKPs family along with hYVH1.

The figure shows the PTPs signature motif in 6 members of MKPs which also are dual

specificity PTPs. Also, it shows that the MKPs motif is almost present in hVH1. In

addition, the figure shows the two invariant residues, D84 and D89, that were mutated

along with D74 (not shown in the figure) to confirm that the D84 is the catalytic

acid/base residue.

* ClustalW software. http://www.ebi.ac.uk/clustalw/

The effect of the D74 mutation on the specific activity of hYVH1 was insignificant. Interestingly, both D84A and D89A mutants lost their phosphatase activity suggesting that both aspartates play an important role in acid/base catalysis. These results revealed the necessity to perform a full pH profile assay for both mutants and compare them with the pH profile of wild type hYVH1.

4.4 Determination of a novel critical residue for acid base catalysis

To explore what role the D84 or D89 mutants play in the catalytic mechanism, kinetic parameters (k_{cat} and K_{cat}/K_m) for D84A and D89A were measured and plotted as a function of pH values in (Fig. 19). The graph showed the apparent loss in pH dependency of D84 suggesting that it is the catalytic acid/base residue. Interestingly, D89A was also almost pH-independent except in pH 4, at which the k_{cat}/K_m value is increased up to approximately equal to the value of k_{cat}/K_m of wild type.

Our hypothesis is that at pH values less than 5, Asp84 is protonated and can function as a catalytic acid. However, at higher pH values Asp84 requires a hydrogen bonding partner (Asp89) to remain protonated. This would explaine the loss of activity at high pH values (>5) for the D89A mutant.

Interestingly, by an alignment between 6 members of MKPs and hYVH1 we found identical corresponding residues for D84 and D89 with the same distance from the active site (Fig. 24). These results suggest that hYVH1 may be a member of the MKPs

65

subfamily, and the hydrogen bonding interaction between these two residues may be critical for acid/base catalysis for MKPs in general.

Ample amounts of GST-hYVH1 protein were subjected to a thrombin-cleavage procedure, purified away from the GST protein, buffer-exchanged, and then sent to Dr. Brian Crane, an X-ray crystallographer at Cornell University. The nature of the interaction between D84 and D89 will be confirmed by the X-ray crystallography structural studies. The tertiary structure will probably resolve the structural settings that may responsible for the low activity of this enzyme. Also, it will reveal the structural relationship between the zinc finger domain and the catalytic domain.

4.5 Detection of activity hYVH1 that expressed in mammalian cells

The low hYVH1 activity that is observed *in vitro* indicates that it requires cellular environment. This environment contains several factors that may regulate hYVH1 phosphatase activity such as localization to membrane, protein-protein interaction, or posttranslation modification. In this study we established a semi *in vivo* assay in which FLAG-tagged hYVH1 was transiently overexpressed in 293 cells, purified using immunoprecipitation, and than added to substrate solution (OMFP or DiFMUP). Although, these experiments are preliminary we achieved expression levels that were detectable by Coomassie Blue from approximately 3 million cells.

This assay can be used to examine hYVH1 over expressed in various eukaryotic cell lines. These cell lines may be subjected to different circumstances that may regulate hYVH1 phosphatase activity. Overall, this *in vivo* assay is a nice complement to the

developed *in vitro* assay that should be useful for deciphering conditions that effect

hYVH1 catalytic activity.

67

FUTURE WORK

Findings from these studies provided technical and mechanistic advances for hYVH1. The technical contribution involves developing enzymatic assays that yielded the first report on the kinetic parameters for hYVH1, while the mechanistic contribution is the identification of a novel critical residue required for the catalytic mechanism of hYVH1.

Prior to quantifying the kinetic parameters, a series of optimization steps were required. This included optimizing the expression hYVH1 in *E.coli*, finding the proper synthetic substrate, and establishing *in vitro/in vivo* phosphatase assays, with which the enzyme can be studied in the future. The *in vitro* assay will be utilized to examine if interacting proteins can regulate hYVH1 activity. For example, Hsp70 has been identified in our lab to interact with hYVH1. Future work will assess the effect of Hsp70 on hYVH1. Also, hYVH1 phosphorylation sites are currently being mapped. Once identified, their effect on hYVH1 activity will be tested using PCR-site directed mutagenesis to create variants that mimic phosphorylation on these sites.

Although the kinetic parameters of hYVH1 are relatively low, they are still within the range of many members of dual specific PTPs such as the mitogen activated protein kinase phosphatase 3 (MKP3), MKP4, or phosphatase of regenerating liver1 (PRL1). However, this low activity suggests that the activity of hYVH1 may need a specific intracellular regulation which is not available in the cellular environment of the bacteria. Therefore, we established a semi-*in vivo* assay to study the activity of the hYVH1 expressed in mammalian cells.

68

Using the *in vivo* assay, our understanding of hYVH1 function will be further broadened by exposing various mammalian cells to different stimuli such phosphatase inhibitors, kinase inhibitors, cell cycle inhibitors, or specific proteins that may interact with hYVH1. The hYVH1 will be immunoprecipitated and subjected to the semi-*in vivo* assay to observe what effect the stimuli has on the activity.

Our mechanistic results started with confirming that hYVH1 is obeying the catalytic mechanism of PTP superfamily. During our attempts to confirm the general acid/base step in the catalytic reaction of hYVH1, we found a residue playing a pivotal role in the general acid/base catalysis of hYVH1. This role is possibly increasing the pKa of the side chain carboxyl of D84, which the catalytic acid/base from 4 up to 6-7. We found that with the mutation of D89 the catalytic reaction will not proceed at physiological pH. Interestingly, in an alignment study we observed a corresponding residue to D89 of hYVH1 in 6 members of dual specificity PTP, specifically from MKPs subfamily, suggesting that this mechanism to increase the pKa of the side chain of the catalytic residue is conserved in MKPs. Also, hYVH1 may be a member of MKPs; this is supported by the presence of MKPs motif in identical corresponding region in hYVH1. However, the role of D89 will be confirmed by an X-ray crystallography study. Also double-mutations in these two residues, D84 and D89, will be a valuable way to be used as a more potent substrate trap.

Recent preliminary data in our lab showed that hYVH1 has an antagonistic function towards apoptosis. This is consistent with the predictive conclusion of the relation of hYVH1 with the MKP subfamily. Further comparison studies between hYVH1 and MKPs in terms of catalytic regulation, structural conformations, and

substrate specificity will lead to a deeper understanding of the physiological function of

this protein, which is conserved from yeast to human.

70

REFERENCES

1. Guan KL, Dixon JE. (1993) Bacterial and viral protein tyrosine phosphatases. *Semin Cell Biol.* 4:389–96.

2. Klumpp S, Krieglstein J. (2002) Phosphorylation and dephosphorylation of histidine residues in proteins. *Eur J Biochem.* 269(4):1067-71.

3. Johnson LN, Barford D.(1993). The effects of phosphorylation on the structures and function of proteins. *Biophys. Biomol. Struct.* 22:199–232.

4. Shirish Shenolikar. (1994) Protein serine/thereonine phosphatase--new avenue for cell regulation. *Annu Rev. Cell Biol.* 10:55—86.

5. Zhong-Yin Zhang. (1998). Protein-tyrosine phosphatases: Biological function, structural characteristics, and mechanism of catalysis. *Critical Reviews in Biochemistry and Molecular Biology,* 33(1):1–52.

6. Alonso A, Sasin J, Bottini N, Friedberg I, Friedberg I, Osterman A, GodzikA, Hunter T, Dixon J, Mustelin T. (2004) Protein tyrosine phosphatases in the human genome.*Cell.*;117(6):699-711.

7. Alexander P. Ducruet, Andreas Vogt, Peter Wipf, and John S. Lazo (2005). Dual specificity protein tyrosine phosphatase: Therapeutic Targets for Cancer and Alzheimer's disease. *Annu Rev Pharmacol Toxicol.* 45:725-50.

8. Hyeongjin Cho, Shawn E. Ramer, Michiyasu Itoh, Eric Kitas, Willi Bannwarth, Paul Burn, Haruo Saito. and Christopher T. Walsh,. (1992) Catalytic Domains of the LAR and CD45 Protein Tyrosine Phosphatases from *Escherichia coli* Expression Systems: Purification and Characterization for Specificity and Mechanism? *Biochemistry*, 31, 133-138.

9. Van Etten R. L,. Ann. N.Y. (1982) Human prostatic acid phosphatase: a histidine phosphatase. *Acad. Sci.* 390: 27-51.

10. Schwartz, J. H., Crestfield, A. M., Lipmann, F.(1963) The amino acid sequence of a tetradecapeptide containing the reactive serine in E.coli alkaline phosphatase. *Proc. Natl. Acad. Sci. USA* 49:722.

11. Barford, D., Flint, A. J., and Tonks, N. K. (1994). Crystal structure of human protein tyrosine phosphatase 1B. *Science* 263: 1397–1404.

12. Daniel L. Lohse, John M. Denu, Nicholas Santoro, and Jack E. Dixon. (1997) Roles of Aspartic Acid-181 and Serine-222 in Intermediate Formation and

Hydrolysis of the Mammalian Protein-Tyrosine-Phosphatase PTP1. *Biochemistry 36,* 4568-4575.

13. Su, X. D., Taddei, N., Stefani, M., Ramponi, G., and Nordlund, P. (1994).The crystal structure of a low-molecular-weight phosphotyrosine protein phosphatase. *Nature* 370: 575–578.

14. Cirri P, Chiarugi P, Camici G, Manao G, Raugei G, Cappugi G, Ramponi G. (1993) The role of Cys12, Cys17 and Arg18 in the catalytic mechanism of low-M(r) cytosolic phosphotyrosine protein phosphatase. *Eur J Biochem.*; 214(3):647-57.

15. Zhang ZY, VanEtten RL. (1991) Pre-steady-state and steady-state kinetic analysis of the low molecular weight phosphotyrosyl protein phosphatase from bovine heart. *J Biol Chem.* 266(3):1516-25.

16. Taddei, N., Chiarugi, P., Cirri, P., Fiaschi, T., Stefani, M., Camici, G., Raugei, G., and Ramponi, G. (1994) Aspartic–129 is an essential residue in the catalytic mechanism of the low M(r) phosphotyrosine protein phosphatase. *FEBS Lett.* 350: 328–332.

17. Zhang, Z., Harms, E., and Van Etten, R. L. (1994) Asp129 of low-molecular-weight protein tyrosine phosphatase is involved in leaving group protonation. *J. Biol. Chem.*269: 25947–25950.

18. Guan, K. L., Broyles, S., and Dixon, J. E.(1991). A Tyr/Ser protein phosphatase encoded by *Vaccinia* virus. *Nature* 350: 359–361.

19. Stuckey, J. A., Schubert, H. L., Fauman, E., Zhang, Z.-Y., Dixon, J. E., and Saper, M. A.(1994). Crystal structure of *Yersinia* protein tyrosine phosphatase at 2.5 Å and the complex with tungstate. *Nature* 370: 571–575.

20. Flint, A. J., Taganis, T., Barford, D., and Tonks, N. K. (1997) Development of "substrate-trapping" mutants to identify physiological substrates of protein tyrosine phosphatases. *Proc. Natl. Acad. Sci.* 94: 1680–1685.

21. Zhang, M., Van Etten, R. L., and Stauffacher, C. V. (1994). Crystal structure of bovine heart phosphotyrosyl phosphatase at 2.2-Å resolution. *Biochemistry* 33: 11097–11105.

22. Yuvaniyama, J., Denu, J. M., Dixon, J. E., and Saper, M. A. (1996). Crystal structure of the dual specificity protein phosphatase VHR. *Science* 272: 1328–1331.

23. Streuli M, Krueger NX, Thai T, Tang M, Saito H. (1990). Distinct functional roles of the two intracellular phosphatase like domains of the receptor-linked protein tyrosine phosphatases LCA and LAR. *EMBO J.* 9:2399–2407.

24. Jia Z, Barford D, Flint AJ, Tonks NK. (1995) Structural basis for phosphotyrosine peptide recognition by protein tyrosine phosphatase 1B. *Science.* 268(5218):1754-8.

25. Nicholas K. TonksS, Curtis D. Diltz, and Edmond H. Fischer. (1988) Characterization of the Major Protein-tyrosine-phosphatases of Human Placenta. *J. Biol. Chem.* 263(14):6731.

26. Jones, S. W., Erikson, R. L., Ingebritsen, V. M., Ingebritsen, T. S. (1989) Phosphotyrosyl-Protein Phosphatases.. *J. Biol. Chem.* 264(13):7747.

27. Pot, D. A., Woodford, T. A., Remboutsika, E., Haun, R. S., Dixon, J. E. (1991) Cloning, Bacterial Expression, Purification, and Characterization of the Cytoplasmic Domain of Rat LAR, a Receptor-like Protein Tyrosine Phosphatase. *J. Biol. Chem.* 266(29):19688.

28. Streuli, M., Kmeger, N. X., Thai, T., Tang, M., Saito, H. (1990) A family of receptor-linked protein tyrosine phosphatases in humans and Drosophila. *EMBO J.* 9(8):2399.

29. Zhang, Z.-Y. (2003) Mechanistic studies on protein tyrosine phosphatases. *Prog. Nucleic Acid Res. Mol. Biol.* 73, 171-220.

30. Gautier J, Solomon MJ, Booher RN, Bazan JF, Kirschner MW. (1991) Cdc25 is a specific tyrosine phosphatase that directly activates p34cdc2. *Cell.* 67(1):197-211.

31. Jonathan B.A.Millar, Clare H.McGowan, Guy Lenaers, Robert Jones and Paul Russell. (1991) p80cdc25 mitotic inducer is the tyrosine phosphatase that activates p34cdc2 kinase in fission yeast. *The EMBO Journal* 10,13, pp.4301 - 4309.

32. KunLiang Guan and Jack E. Dixon. (1991) Evidence for Protein-tyrosine-phosphatase Cysteine-Phosphate Intermediat. *J. Biol. Chem.* 266, 26, PP. 17026-17030.

33. Zhou G, Denu JM, Wu L, Dixon JE. The catalytic role of Cys124 in the dual specificity phosphatase VHR. J Biol Chem. 1994 Nov 11;269(45):28084-90.

34. Johnson P, Ostergaard HL, Wasden C, Trowbridge IS. (1992) Mutational analysis of CD45. A leukocyte-specific protein tyrosine phosphatase. *J. Biol. Chem.* 267(12):8035-41.

35. Johnson P, Ostergaard HL, Wasden C, Trowbridge IS. (1992) Mutational analysis of CD45. A leukocyte-specific protein tyrosine phosphatase. *J. Biol. Chem.* 267(12):8035-41.

36. Zhong-Yin Zhang,, Bruce A. Palfey,s Li W u , and Yu Zhao. (1995) Catalytic Function of the Conserved Hydroxyl Group in the Protein Tyrosine Phosphatase Signature Motif. *Biochemistry 34,* 16389- 16396.

37. Dunphy, W. G. and Kumagai, A. (1991) The cdc25 protein contains an intrinsic phosphatase activity. *Cell* 67: 189–196.

38. Gregoret, L. M., Rader, S. D., Fletterick, R. J., and Cohen, F. E. (1991) Hydrogen bonds involving sulfur atoms in proteins. *Prot.: Struct., Funct., Genet.* 9: 99–107.

39. Flint, A. J., Taganis, T., Barford, D., and Tonks, N. K. (1997) Development of "substrate-trapping" mutants to identify physiological substrates of protein tyrosine phosphatases. *Proc. Natl. Acad. Sci.* 94: 1680–1685.

40. Zhang ZY, Malachowski WP, Van Etten RL, Dixon JE. (1994) Nature of the rate-determining steps of the reaction catalyzed by the Yersinia protein-tyrosine phosphatase. *J Biol Chem.* 269(11):8140-5.

41. Guan KL, Dixon JE. (1990) Protein tyrosine phosphatase activity of an essential virulence determinant in Yersinia. *Science.* 249(4968):553-6.

42. Zhang ZY, Wang Y, Dixon JE. (1994) Dissecting the catalytic mechanism of protein-tyrosine phosphatases. *Proc Natl Acad Sci*. 91(5):1624-7.

43. Zhang, M., Van Etten, R. L., and Stauffacher, C. V. (1994) Crystal structure of bovine heart phosphotyrosyl phosphatase at 2.2-Å resolution. *Biochemistry* 33: 11097–11105.

44. McCain DF, Catrina IE, Hengge AC, Zhang ZY. (2002) The catalytic mechanism of Cdc25A phosphatase. *J Biol Chem*. 277(13):11190-200.

45. Wen Chen, Manuel Wilborn, and Johannes Rudolph. (2000) Dual-Specific Cdc25B Phosphatase: In Search of the Catalytic Acid. *Biochemistry*, 39, 10781-10789.

46. Johannes Rudolph. (2002) Catalytic Mechanism of Cdc25. *Biochemistry*, *41*, 14613-14623.

47. Jia, Z., Barford, D., Flint, A. J., and Tonks, N. K. (1995) Structural basis for phosphotyrosine peptide recognition by protein tyrosine phosphatase1B. *Science* 268: 1754–1758.

48. Hakes DJ, Martell KJ, Zhao WG, Massung RF, Esposito JJ, Dixon JE. (1993) A protein phosphatase related to the vaccinia virus VH1 is encoded in the

genomes of several orthopoxviruses and a baculovirus. *Proc Natl Acad Sci.*
90(9):4017-21.

49. Guan K, Hakes DJ, Wang Y, Park HD, Cooper TG, Dixon JE. (1992) A yeast
protein phosphatase related to the vaccinia virus VH1 phosphatase is induced
by nitrogen starvation. *Proc Natl Acad Sci.* 89(24):12175-9.

50. Beeser AE, Cooper TG.(1999) The dual-specificity protein phosphatase Yvh1p
acts upstream of the protein kinase mck1p in promoting spore development in
Saccharomyces cerevisiae. *J Bacteriol.* 181(17):5219-24.

51. Beeser AE, Cooper TG.(2000) The dual-specificity protein phosphatase Yvh1p
regulates sporulation, growth, and glycogen accumulation independently of
catalytic activity in Saccharomyces cerevisiae via the cyclic AMP-dependent
protein kinase cascade. *J Bacteriol.* 182(12):3517-28.

52. Muda M, Manning ER, Orth K, Dixon JE. (1999) Identification of the human
YVH1 protein tyrosine phosphatase orthologue reveals a novel zinc binding
domain essential for in vivo function. *J Biol Chem.* 274(34):23991-5.

53. Leon O, Roth M. (2000) Zinc fingers: DNA binding and protein-protein
interactions. Biol Res. 2000;33(1):21-30. *Review. Erratum in: Biol Res.*
33(2):185.

54. Sakumoto N, Yamashita H, Mukai Y, Kaneko Y, Harashima S. (2001) Dual-specificity protein phosphatase Yvh1p, which is required for vegetative growth and sporulation, interacts with yeast pescadillo homolog in Saccharomyces cerevisiae. *Biochem Biophys Res Commun.* 289(2):608-15.

55. Kumar R, Musiyenko A, Cioffi E, Oldenburg A, Adams B, Bitko V, Krishna SS, Barik S. (2004) A zinc-binding dual-specificity YVH1 phosphatase in the malaria parasite, Plasmodium falciparum, and its interaction with the nuclear protein, pescadillo. *Mol Biochem Parasitol.* 133(2):297-310.

56. Forus A, Berner JM, Meza-Zepeda LA, Saeter G, Mischke D, Fodstad O, Myklebost O. Molecular characterization of a novel amplicon at 1q21-q22 frequently observed in human sarcomas. Br J Cancer. 1998 Aug;78(4):495-503.

57. Forus A, Weghuis DO, Smeets D, Fodstad O, Myklebost O, van Kessel AG. Comparative genomic hybridization analysis of human sarcomas: I. Occurrence ofgenomic imbalances and identification of a novel major amplicon at 1q21-q22 insoft tissue sarcomas.Genes Chromosomes Cancer. 1995 Sep;14(1):8-14.

58. Kresse SH, Berner JM, Meza-Zepeda LA, Gregory SG, Kuo WL, Gray JW, Forus A, Myklebost O. (2005) Mapping and characterization of the amplicon near APOA2 in 1q23 in human sarcomas by FISH and array CGH. *Mol Cancer.* 4:39.

59. Wang WQ, Bembenek J, Gee KR, Yu H, Charbonneau H, Zhang ZY. (2004) Kinetic and mechanistic studies of a cell cycle protein phosphatase Cdc14. J Biol Chem. 2004 Jul 16;279(29):30459-68.

60. Sun JP, Wang WQ, Yang H, Liu S, Liang F, Fedorov AA, Almo SC, Zhang ZY. (2005) Structure and biochemical properties of PRL-1, a phosphatase implicated in cell growth, differentiation, and tumor invasion. Biochemistry. 44(36):12009-21.

61. Gottlin EB, Xu X, Epstein DM, Burke SP, Eckstein JW, Ballou DP, Dixon JE. (1996) Kinetic analysis of the catalytic domain of human cdc25B. J Biol Chem. 271(44):27445-9.

62. Zhou B, Zhang ZY.(1999) Mechanism of mitogen-activated protein kinase phosphatase-3 activation by ERK2. J Biol Chem. 274(50):35526-34.

63. Jeong DG, Yoon TS, Kim JH, Shim MY, Jung SK, Son JH, Ryu SE, Kim SJ.(2006) Crystal Structure of the Catalytic Domain of Human MAP Kinase Phosphatase 5:Structural Insight into Constitutively Active Phosphatase. J Mol Biol. 360(5):946-55. Epub 2006 Jun 9.

VITA AUCTORIS

Name: **KHALED EMOSRATI**

Place & Date of Birth: Tripoli – Libya . 05, June. 1969

Education:	2004-2006	University of Windsor Windsor, Ontario, Canada Department of Chemistry & Biochemistry M.Sc. Candidate, Biochemistry
	1997-1998	University of Al-Fatah Tripoli, Libya Department of Medical Laboratories Science B.Sc. Medical Laboratories Science
	1989-1992	University of Al-Fatah Tripoli, Libya Department of Medical Laboratories Science Higher Diploma. Medical Laboratories Science